TI Designs

SONAR Receiver Path Sub-System Reference Design Using the AFE5809

TI Designs

TI Designs provide the foundation that you need including methodology, testing and design files to quickly evaluate and customize the system. TI Designs help *you* accelerate your time to market.

Design Resources

AFE5809	Product Folder
TSW1400EVM	Product Folder

TI E2E™ Community — ASK Our E2E Experts

Design Features

- Capable of Measuring SONAR Signals From 30 kHz to 32.5 MHz
- Digital Demodulator for Envelope Detection and Beamforming
- Variable Sample Frequency 10 to 65 MSPS With External Clock Capability
- Variable Gain settings With a –4- to 54-dB Range
- Variable Input Impedance Settings
- Tested and Provides Design Reference Materials Including Schematics and BOM

Featured Applications

- SONAR
- Ultrasound with Beamforming
- High-Speed Data Acquisition

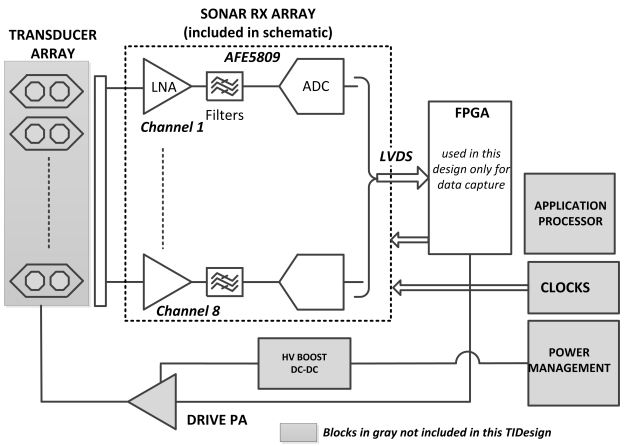

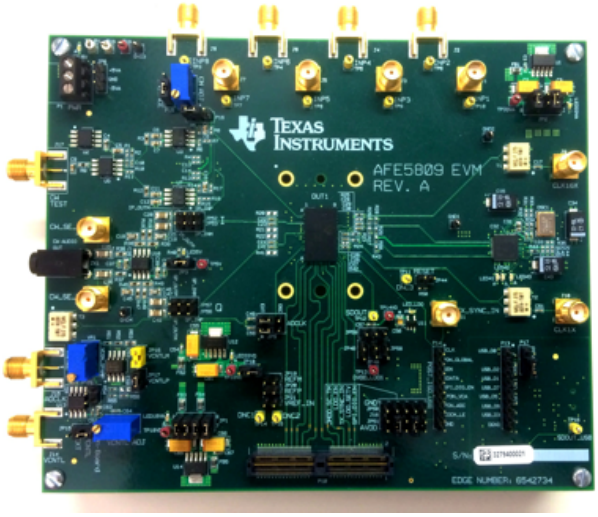

An IMPORTANT NOTICE at the end of this TI reference design addresses authorized use, intellectual property matters and other important disclaimers and information.

All trademarks are the property of their respective owners.

Copyright © 2015, Texas Instruments Incorporated

1 Introduction

This reference design demonstrates a possible 8-channel SONAR receive path sub-circuit. Included in the design are theory of operation, schematics, bill of materials and initial measurement data to substantiate theory.

The scope of this document is to exhibit how TI's high performance analog front end, AFE5809, is ideal for use in low, mid and high-end SONAR systems as well as high-end ultrasound systems. The AFE5809 greatly simplifies conventional system integration by providing eight channels of Low Noise Amplifier, VCA, ADC, I/Q demodulator, and decimator. This reference design demonstrates how this ASIC-based solution yields the high performance requirements of SONAR and ultrasound systems while reducing back-end computational requirements. Beamforming, an imaging technique employed in both SONAR and B-mode ultrasound technologies, requires envelope detection. Envelope detection is performed by I/Q demodulating the digitized signal into its in-phase and quadrature components, and then decimating the result. By processing this before serialization, and supplying already demodulated and decimated data at the interface to the system back-end, the AFE5809 can reduce the high data rate at this interface and absorb the envelope detection functionality, a necessary component of the digital beamforming downstream in the signal chain.

This document is organized as follows: Section 2 presents a brief overview of SONAR systems and corresponding requirements. Section 3 analyzes beamforming and presents theory on the phase rotation that can be applied to analyze/ measure multi-channel data. Section 4 presents key features of the AFE5809 with an emphasis on those that are more suitable for multi-channel SONAR RX signal processing. Section 5 outlines the test set up and measurement methodology that was used and actual measurement data emulating the use of the AFE5809 in SONAR applications is presented in Section 6.

2 SONAR Overview

SONAR, an acronym for SOund Navigation And Ranging, refers to the method of using sound waves in an underwater environment to detect and map objects. Typical SONAR systems use ultrasonic signals whose frequencies typically range upwards from 20 kHz all the way to 800kHz. Applications of SONAR are widespread including bathymetry (or the study of oceans floors), vessel navigation, search and rescue (SAR), structural inspections such as pipelines, and recreational and commercial fish locators.

SONAR systems fall into two categories: active and passive. Passive systems are listening systems in which no signal is transmitted and are generally needed when the listener wants to remain undetectable, such as some military vessels. Conversely, active SONAR systems make use of a transmitted signal, called a "ping", originating from a transmitter element array located near the receiver or a combined transmit/receive element. If an object in the field of interest such as vessel or school of fish is encountered by the transmitted wave, an attenuated and distorted reflection of this transmitted signal, called the "echo", propagates back towards the transduce. The receive element in the transducer converts this acoustic echo into an electrical voltage, and subsequent signal chain circuitry processes the signal. Because this echo is so attenuated in the medium, and because of the wide range of signal amplitudes expected from far, near and moving objects, the echo will require not only amplification before digitization, but also a large dynamic range to accommodate this variability and maximize the resolution of the digitized signal. The primary goal of the receiver is to decide where the received signal originated. The threshold for this decision is primarily dependent on the signal-to-noise ratio (SNR) of the system.

Like most modern communication systems, there are methods for improving the SNR of a SONAR system. These methods can be found in both the analog and digital domains and are employed to increase quality or the range over which the system can be used. A typical SONAR system comprises a transducer whose I/O switches between a transmit chain and a receiver chain. A typical receive chain conditions the signal with variable-gain analog amplifiers and filters so that the dynamic range of the ADC is maximized before digitizing the signal. The low-pass filter before the ADC acts as an anti-aliasing filter, which limits the higher-order harmonics and high-frequency noise that gets folded back, or aliased, into the first Nyquist zone. This filter is typical and recommended for most ADC applications.

In the digital domain, decimation and filtering can be used to further improve SNR as well as reduce data rates to lessen the processing burden on the FPGA or back-end DSP. In addition, spatial filtering can be employed to provide directivity to the transmitted ping through beam forming. Such methods control phase and amplitudes of multiple channels to create constructive interference on the transmitted signal. The receiver employs similar tactics by sensing the echo on multiple sensors.

Copyright © 2015, Texas Instruments Incorporated

3 Beamforming Overview

In SONAR systems and B-mode ultrasound, acoustic waves centered around a particularly frequency are transmitted into the imaging medium, and the echoed waves are received and recorded as a function of time and position. Because the transmission and reception of sound waves are performed at the same location (that is, at the transducer probe), the distances through which these waves propagate can be computed through simple trigonometric geometry. This concept is schematically represented in Figure 1.

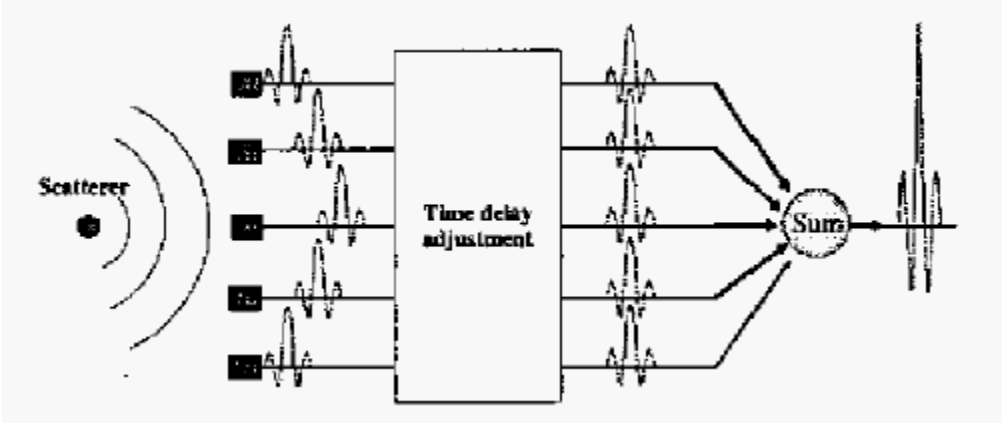

Figure 1. Principle of Delay-and-Sum Beamforming [2]

Copyright © 2015, Texas Instruments Incorporated

In Figure 2, the red arrow represents the distance covered by the transmit and receive waves from one transducer element, whereas the pink arrow represents the propagation distance from a second, neighboring element to the same location in the imaging medium. The waveforms received by different transducer elements constitute independent data channels. Evidently, these distances are unequal, and assuming a constant speed of sound in the medium, the propagation times are also different.

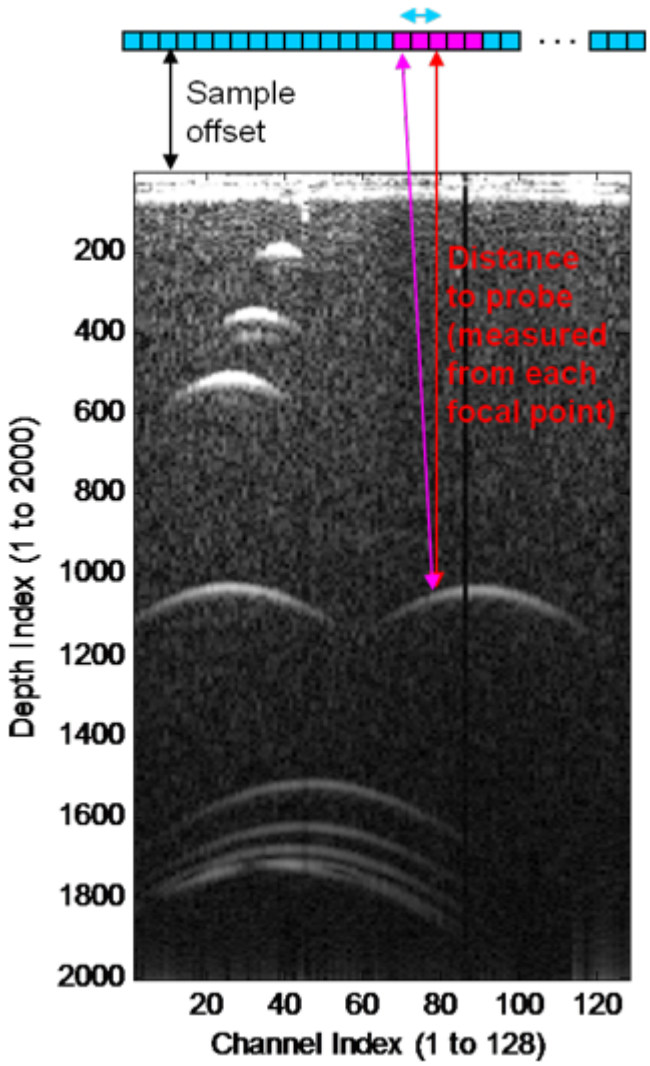

Figure 2. Geometry of Propagation Paths

Copyright © 2015, Texas Instruments Incorporated

The SNR of the received echoes tends to be low due to:

- the attenuation of the acoustic wave in the medium
- the limited power output for wave transmitted by transducer

To mitigate the low SNR, received echoes of multiple neighboring channels are combined through beamforming. The difference in propagation time between neighboring channels is dictated by the physical location of the transducer elements relative to the point in the imaging medium for which beamforming is performed. Therefore, this time difference is computed and the corresponding channel data is delayed in time and cumulatively summed for higher SNR. This summation requires that the signal noise from all elements is correlated, which will therefore result in destructive summation for this noise.

To apply the delay, the absolute propagation time difference is decomposed into two components:

- integer delay: portion of delay that aligns with an ADC clock edge, or an integer multiple of the ADC clock period
- fractional delay: the remaining component after the integer delay portion is subtracted from the total time delay, expressed as a fraction of the ADC clock period

The example signal in Figure 3 illustrates the distinction between integer and fractional delay. At a sampling frequency of 40 MHz, the period between actual data samples (represented by the vertical arrows) is 1/40 MHz = 25 ns. Given that the signal needs to be delayed by an arbitrary time, say 106.25 ns, it is possible to locate the closest data sample to approximate the delayed value. In this case, floor (106.25 ns/25 ns) = 4, meaning the fourth sample is selected to approximate the delayed value. For higher accuracy, some interpolation can be done on the neighboring samples. Assuming that an implementation has the resolution of ¼ clock period, the signal amplitude at the first tick mark on the right of the fourth sample can be approximated using interpolation techniques.

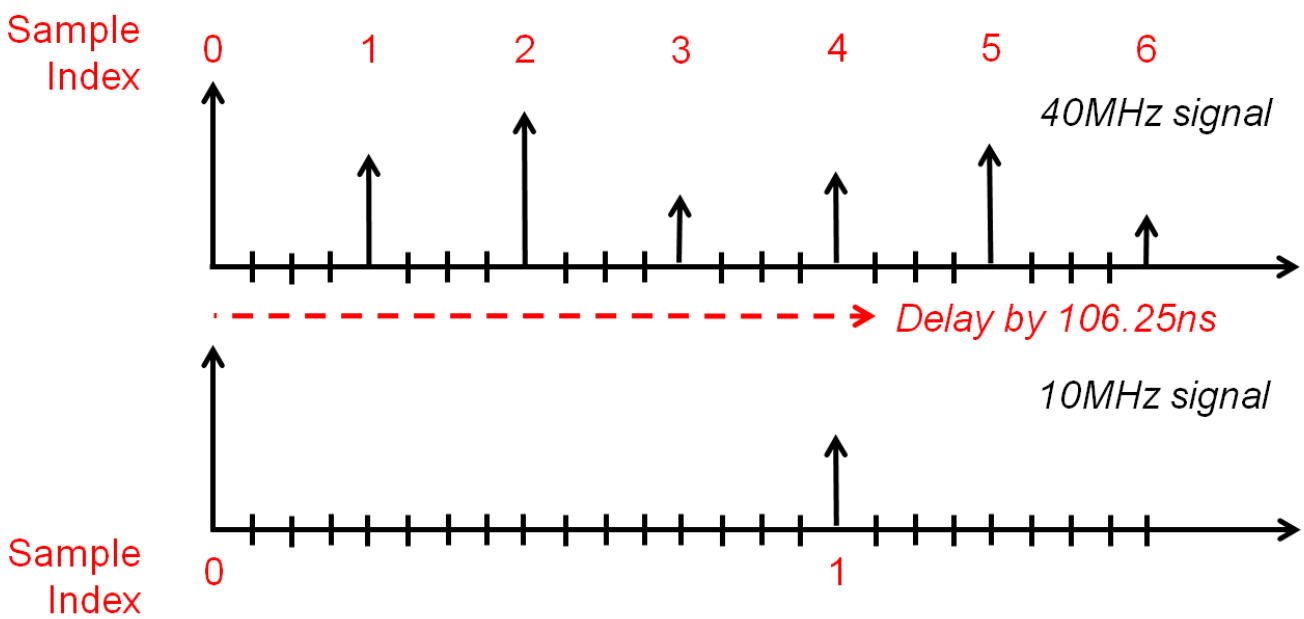

Figure 3. Schematic of Integer versus Fractional Delay

Copyright © 2015, Texas Instruments Incorporated

The integer delay is first applied on the output of the ADC by selecting the appropriate data sample corresponding to that number of cycles worth of delay. The fractional delay can be implemented either using an interpolation filter or a phase rotator, which is applied on the output of the integer delay block. The resulting delayed channel data are then summed and fed to an envelope detection block. This beamformer structure is schematically shown in Figure 4.

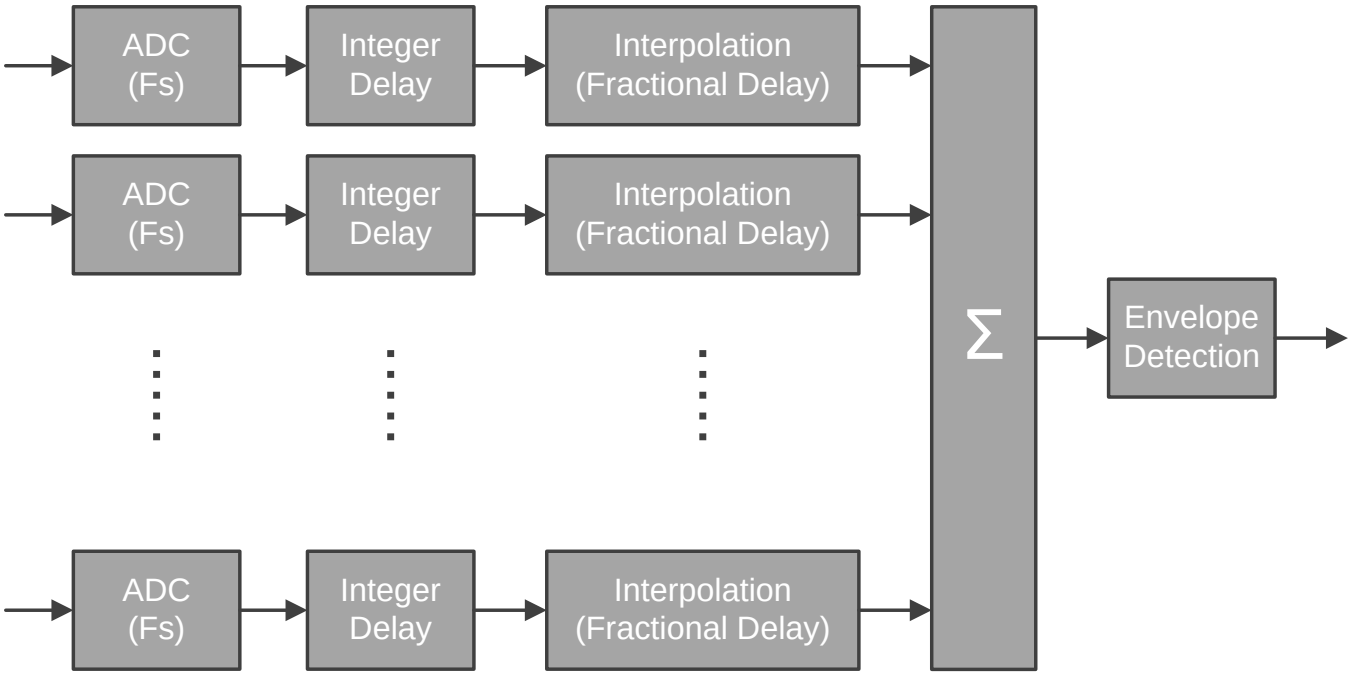

Figure 4. Conventional Time-Delay Beamformer Block Diagram

Copyright © 2015, Texas Instruments Incorporated

3.1 Envelope Detection

Once the appropriately delayed channel data is combined through summation, the peaks in the resulting signal are identified through envelope detection. The data rate resulting a lower frequency signal can then be further reduced through log compression, which provides the pixel values finally displayed as an ultrasound image. A common implementation of envelope detection can be described in two steps: I-Q demodulation followed by decimation. This section outlines the mathematical derivations for these two processing steps.

3.1.1 I-Q Demodulation

Any signal waveform can be decomposed into its in-phase and quadrature components:

$$x_n(t) = I(t)\cos(\omega_c t) + Q(t)\sin(\omega_c t) \tag{1}$$

Assuming the signal to be amplitude modulated (that is, some low-frequency envelope modulated at a higher carrier frequency), the following derivation decomposes $x_n(t)$ into I(t) and Q(t).

$$x_n(t) = A(t)\cos(\omega_c t + \varphi(t)) \tag{2}$$

$$x_n(t) = A(t)\cos(\varphi(t) + \omega_c t) = A(t)\sin\left(\varphi(t) + \frac{\pi}{2} + \omega_c t\right)$$

$$x_n(t) = \left[A(t)\sin\left(\varphi(t) + \frac{\pi}{2}\right)\right]\cos(\omega_c t) + \left[A(t)\cos\left(\varphi(t) + \frac{\pi}{2}\right)\right]\sin(\omega_c t) \tag{3}$$

Comparing Equation 1 and Equation 3, one can extract the expressions for the in-phase and quadrature components, I(t) and Q(t):

$$I(t) = A(t)\sin\left(\varphi(t) + \frac{\pi}{2}\right) = A(t)\cos(\varphi(t)) \tag{4}$$

$$Q(t) = A(t)\cos\left(\varphi(t) + \frac{\pi}{2}\right) = -A(t)\sin(\varphi(t)) \tag{5}$$

Rewriting the expression in Equation 2, one can represent the same signal as the product of the envelope signal $\overline{x_n}(t)$ and the cosine at carrier frequency ω_c, shown here in complex exponential form:

$$x_n(t) = \frac{1}{2}\left(\widetilde{x_n}(t) \times e^{j\omega_c t} + \widetilde{x_n}^*(t) \times e^{-j\omega_c t}\right) \tag{6}$$

Expanding Equation 1 in complex exponential form yields:

$$x_n(t) = \frac{I(t)}{2}\left(e^{j\omega_c t} + e^{-j\omega_c t}\right) + \frac{Q(t)}{2j}\left(e^{j\omega_c t} - e^{-j\omega_c t}\right)$$

$$x_n(t) = \frac{I(t)}{2}\left(e^{j\omega_c t} + e^{-j\omega_c t}\right) - j\frac{Q(t)}{2}\left(e^{j\omega_c t} - e^{-j\omega_c t}\right)$$

$$x_n(t) = \frac{1}{2}\left[\left(I(t) - jQ(t)\right) \times e^{j\omega_c t} + \left(I(t) + jQ(t)\right) \times e^{-j\omega_c t}\right] \tag{7}$$

The expression for the complex-valued envelope signal $\overline{x_n}(t)$ in terms of the I-Q components can be obtained by comparing Equation 2 and Equation 3:

$$\Rightarrow \widetilde{x_n}(t) = I(t) - jQ(t) \tag{8}$$

Equation 9 shows that the envelope signal can be reconstructed by taking the absolute value of a complex function where the real and imaginary parts are the in-phase and quadrature components, respectively:

$$\Rightarrow \left|\widetilde{x_n}(t)\right| = \left|I(t) - jQ(t)\right| = \sqrt{I^2(t) + Q^2(t)} \tag{9}$$

The relationship in Equation 9 can be exploited to use I-Q demodulation as a method of envelope detection.

Copyright © 2015, Texas Instruments Incorporated

3.1.2 Decimation

Since the demodulated signals (I and Q parts) are of a much lower frequency compared to the high carrier frequency, the same signal can be represented at a much lower sampling rate than the one used for the total modulated signal (represented in Equation 1). This allows data reduction through down-sampling.

The Shannon-Nyquist sampling theorem states that any signal can be exactly reconstructed from its sampled version as long as the original signal only contains frequencies at or below one-half of the sampling rate. This criterion must still be maintained after down-sampling to avoid aliasing. An anti-aliasing filter is typically used to ensure the demodulated signals are still sampled at the Nyquist rate. For a given decimation factor M, the demodulated signals should be passed through a low-pass filter with frequency cutoff at π/M. The combined effect of the anti-aliasing filter (with cutoff at π/M) followed by downsampling by a factor of M constitutes decimation.

The overall block diagram representing the envelope detection processing unit is shown in Figure 5, where the input x[n] is the amplitude modulated signal from which envelope information is to be extracted, and the outputs Idec[n] and Qdec[n] can be combined to obtain the absolute value of the complex-valued envelope signal. For an example input signal sampled at 40 MHz, the effective data rate is reduced by 50% for a decimation factor of 4.

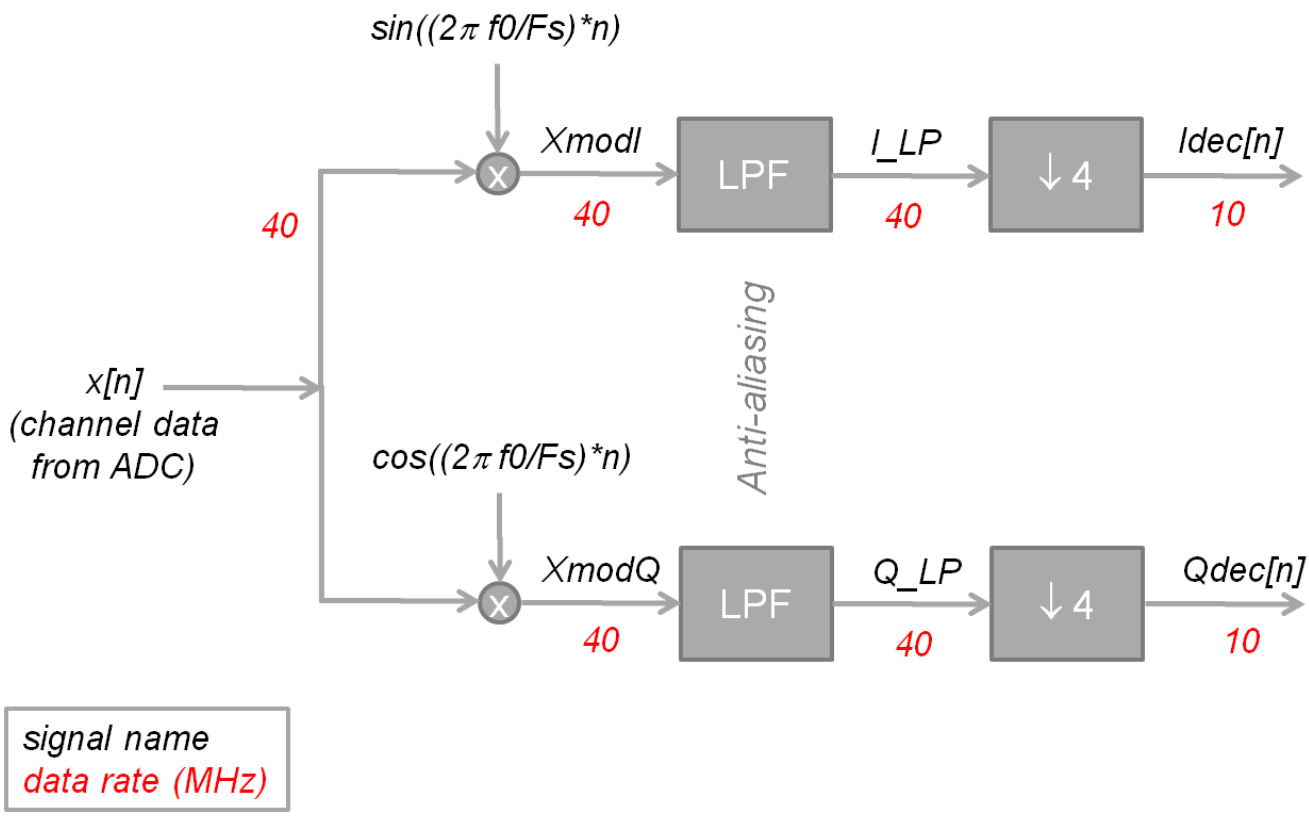

Figure 5. Envelope Detector Block Diagram

Copyright © 2015, Texas Instruments Incorporated

3.2 Beamforming Demodulated Data

As discussed in Section 1, the digitized channel data is supplied by the ADCs to the beamformer at a very high rate. Assuming an ADC sampling frequency of 40 MHz and an ADC resolution of 14 bits, the data rate comes to 560 MSPS. A reduction in data rate at the interface between ADC and beamformer allows for easier system integration.

The envelope detection block in Figure 2 allows for data reduction after summation of channel data, an alternate system architecture that moves this processing block to the left of the beamformer is desirable for the following reasons:

- Envelope detection is a necessary processing step downstream in the beamformer, so having this functionality in the AFE effective reduces the processing performed by the beamformer; and
- As noted in Section 3.1, the envelope detection block effectively reduces data rate by a factor of M / 2, as long as M > 2 (since demodulation into I-Q components effective doubles the data rate while holding sampling frequency constant).

This work explores an alternate implementation of the system. In this alternate setup, shown in Figure 6, the demodulation and decimation steps are performed by the AFE5809, such that the output signals provided to the beamformer are the decimated versions of the in-phase and quadrature components of channel data.

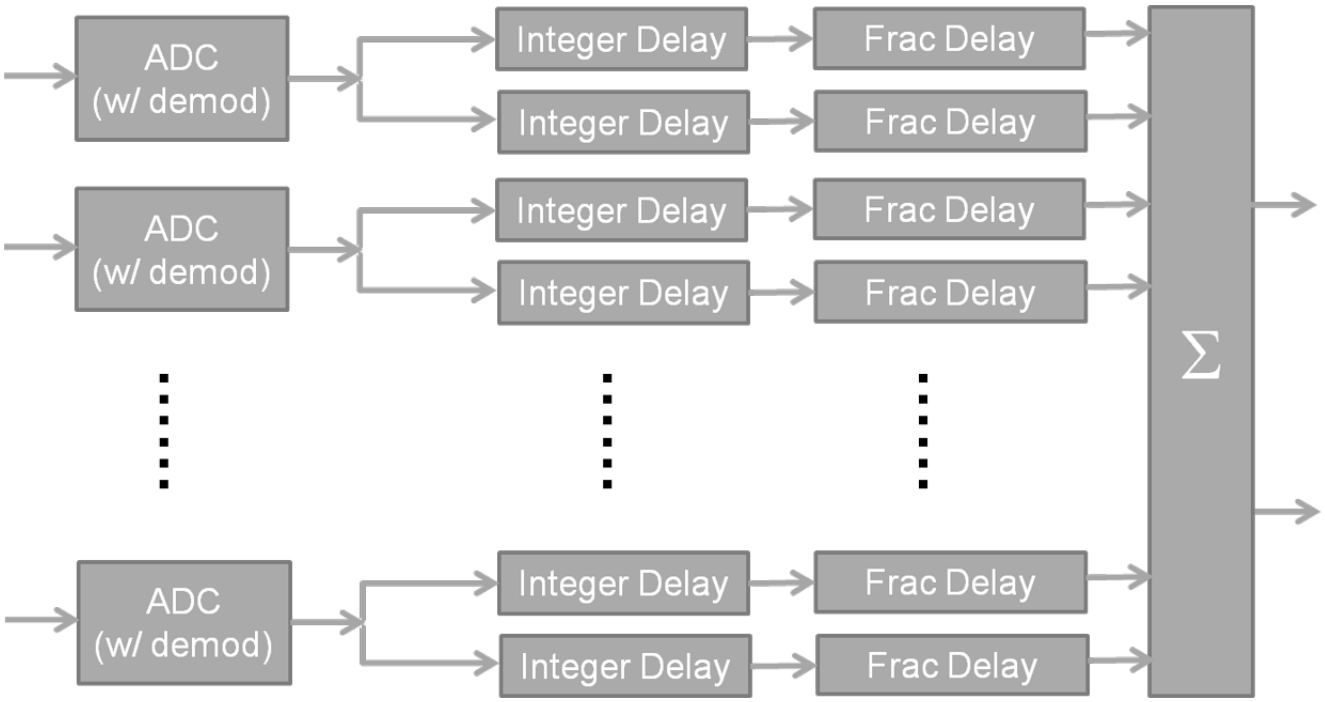

Figure 6. Time-Delay Beamformer for Demodulated Channel Data [2]

Note that because the I and Q channel data provided to the beamformer is now sampled at a lower frequency, the integer delay block now supports a coarser resolution of delay values (each sampling period is now longer) and the accuracy requirement of the fractional delay is more severe. To meet this requirement, phase rotation beamforming is considered.

Copyright © 2015, Texas Instruments Incorporated

3.3 Phase Rotation Beamforming

Figure 7 schematically shows the comparison between delaying the original higher frequency signal and delaying the 4× downsampled signal by the same amount. To delay by 106.25 ns, the 40-MHz signal needs to be delayed by 4 and 1/4 clock cycles, whereas the 10-MHz signal needs to be delayed by 1 and 1/16 cycles.

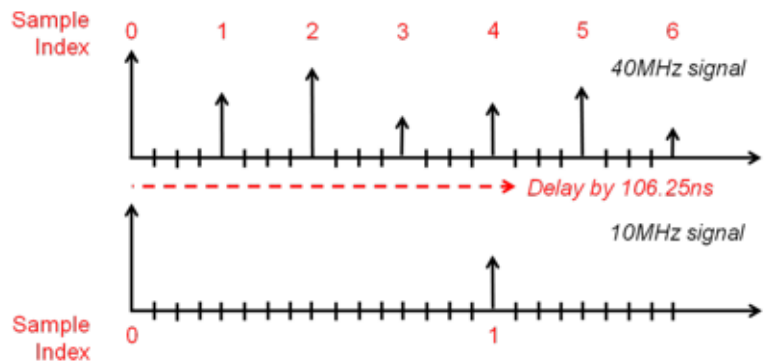

Figure 7. Schematic Comparison of Delaying 40-MHz and 10-MHz Signals

Because the available data samples are spaced farther apart in time, the amount of interpolation necessary to achieve the same delay resolution (6.25 ns) goes from quarter cycle to 1/16th of a cycle. Phase rotation is explored in this section as a method of compensating for the reduced number of samples available for integer delay.

In general, a time delay can be applied in the frequency domain instead of the time domain. Using Fourier transforms, one can leverage the mapping from a shift in the time domain to a multiplication by a complex exponential in the frequency domain:

$$f(t-\tau) \leftrightarrow \mathcal{F}(\omega)e^{-j\omega\tau} \tag{10}$$

Applying a time delay of τ_n to the expression for the nth channel data expressed in Equation 6:

$$x_n(t-\tau_n) = \frac{1}{2}\left(\widetilde{x_n}(t-\tau_n)\times e^{j\omega_c(t-\tau_n)} + \widetilde{x_n}^*(t-\tau_n)\times e^{-j\omega_c(t-\tau_n)}\right) \tag{11}$$

Expanding the complex exponentials:

$$x_n(t-\tau_n) = \frac{1}{2}\left(e^{-j\omega_c\tau_n}\times\left[\widetilde{x_n}(t-\tau_n)\times e^{j\omega_c t}\right] + e^{+j\omega_c\tau_n}\times\left[\widetilde{x_n}^*(t-\tau_n)\times e^{-j\omega_c t}\right]\right)$$

Applying the time-shift property shown in Equation 10 along with the complex conjugation and multiplication by complex exponential in the time domain (dual of the time-shift property), listed here:

$$f^*(t) \leftrightarrow \mathcal{F}^*(-\omega)$$

$$e^{j\omega_c t}\times f(t) \leftrightarrow \mathcal{F}(\omega-\omega_c)$$

$$x_n(t-\tau_n) = \frac{1}{2}\mathcal{F}^{-1}\left(\begin{array}{c} e^{-j\omega_c\tau_n}\times F\left[\widetilde{x_n}(t-\tau_n)\times e^{j\omega_c t}\right] \\ +e^{+j\omega_c\tau_n}\times F\left[\widetilde{x_n}^*(t-\tau_n)\times e^{-j\omega_c t}\right]\end{array}\right) \tag{12}$$

Copyright © 2015, Texas Instruments Incorporated

$$x_n(t-\tau_n) = \frac{1}{2}\mathcal{F}^{-1}\left(e^{-j\omega_c\tau_n} \times \widetilde{X_n}(\omega-\omega_c) \times e^{-j(\omega-\omega_c)\tau_n} + e^{+j\omega_c\tau_n} \times \widetilde{X_n}^*(\omega-\omega_c) \times e^{+j(\omega-\omega_c)\tau_n}\right)$$

$$x_n(t-\tau_n) = \frac{1}{2}\mathcal{F}^{-1}\left(e^{-j\omega\tau_n} \times \widetilde{X_n}(\omega-\omega_c) + e^{+j\omega\tau_n} \times \widetilde{X_n}^*(\omega-\omega_c)\right) \quad (13)$$

Equation 13 forms the basis of frequency domain beamforming. Taking the Fourier transform of channel data $x_n(t)$, one would apply the delay of τ_n by multiplication of a complex exponential and a frequency shift, then take the inverse Fourier transform to obtain the delayed signal $x_n(t - \tau_n)$. However, the hardware cost of taking the forward and reverse fast Fourier Transform is significant, and the large amount of memory required corresponds to the DFT size.

By applying the narrowband signal assumption such that the approximations $\omega t \approx \omega_c t$ and $\omega\tau_n \approx \omega_c t_n$ can be made, Equation 13 yields the special case of phase rotation beamforming expressed as:

$$x_n(t-\tau_n) = \frac{1}{2}\mathcal{F}^{-1}\left(e^{-j\omega_c\tau_n} \times \widetilde{X_n}(\omega-\omega_c) + e^{+j\omega_c\tau_n} \times \widetilde{X_n}^*(\omega-\omega_c)\right) \quad (14)$$

To demonstrate the ability to delay a signal using phase rotation, an example waveform is defined in MATLAB and processed shown in Figure 8 (adapted from *Software-based Ultrasound Phase Rotation Beamforming on Multi-core DSP* [SPRABO1]). A Gaussian envelope modulated by a sinusoidal signal of 5 MHz forms the original (blue) waveform, and a time-offset copy of this waveform is plotted in red at the top of Figure 9. The two signals, denoted by $u_1[m]$ and $u_2[m]$, are defined such that $u_2[m]$ is an exact copy of $u_1[m]$ that leads $u_1[m]$ by 25 ns. The larger delay resolution is selected for demonstration purposes, and smaller delay values can be fulfilled using the same algorithm.

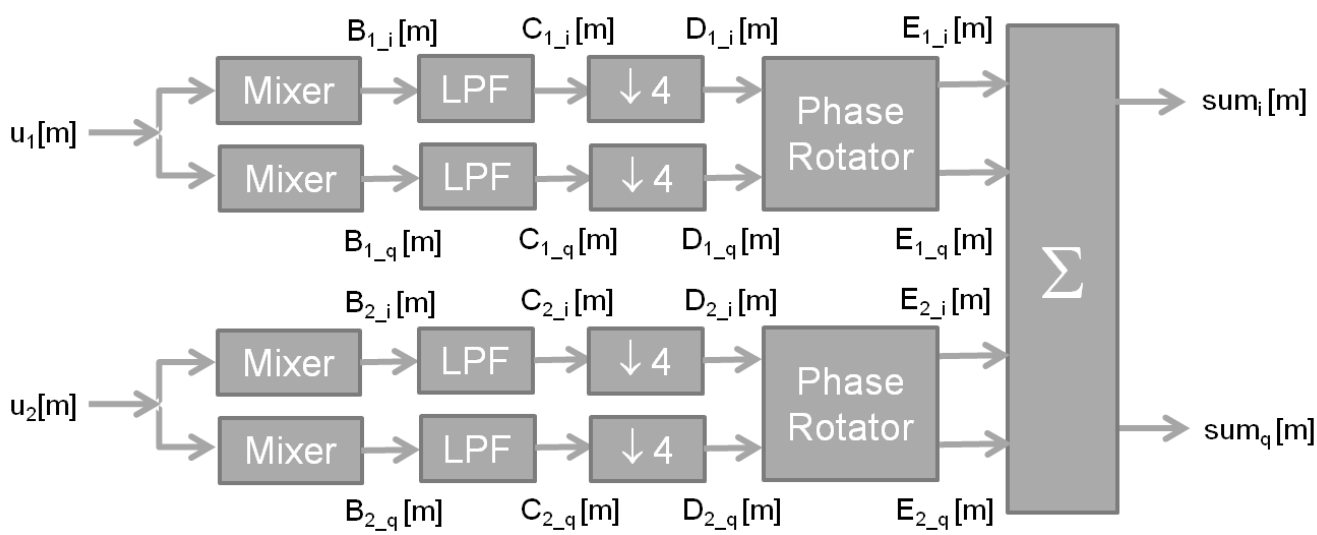

Figure 8. Block Diagram for Phase Rotator Functionality Verification

Copyright © 2015, Texas Instruments Incorporated

After a mixer (demodulating into I and Q parts), followed by an anti-aliasing filter and a decimation by a factor of 4, the red and blue signals shown in the second plot in Figure 9 represent the absolute values of complex signals formed from $D_{1_i}[m]$ and $D_{1_q}[m]$ (blue), and $D_{-2_i}[m]$ and $D_{2_q}[m]$ (red), respectively. These waveforms are taken to be the envelope signals for $u_1[m]$ and $u_2[m]$ based on the relationship summarized in Equation 9. The green curve superimposed on the same plot shows the absolute value of the complex sum expressed here:

$$\left|\left(D_{1_i}[m]+D_{2_i}[m]\right)+\left(D_{1_q}[m]+D_{2_q}[m]\right)\right| = \sqrt{\left(D_{1_i}[m]+D_{2_i}[m]\right)^2+\left(D_{1_q}[m]+D_{2_q}[m]\right)^2} \tag{15}$$

The phase rotators in Figure 8 perform the operation on complex values described here in complex and matrix form:

$$E_1 = e^{-j\omega_c\tau_n} \times D_1 \tag{16}$$

$$\begin{bmatrix} E_{1_i} \\ E_{1_q} \end{bmatrix} = \begin{bmatrix} \cos(\omega_c\tau_n) & \sin(\omega_c\tau_n) \\ -\sin(\omega_c\tau_n) & \cos(\omega_c\tau_n) \end{bmatrix} \times \begin{bmatrix} D_{1_i} \\ D_{1_q} \end{bmatrix} \tag{17}$$

The waveforms for the absolute values of the complex signals constructed from $E_{1_i}[m]$ and $E_{1_q}[m]$ (blue), and $E_{2_i}[m]$ and $E_{2_q}[m]$ (red), are shown in the bottom plot in Figure 9. The green curve in this plot represents the absolute value of the following complex sum:

$$\left|\left(E_{1_i}[m]+E_{2_i}[m]\right)+\left(E_{1_q}[m]+E_{2_q}[m]\right)\right| = \sqrt{\left(E_{1_i}[m]+E_{2_i}[m]\right)^2+\left(E_{1_q}[m]+E_{2_q}[m]\right)^2} \tag{18}$$

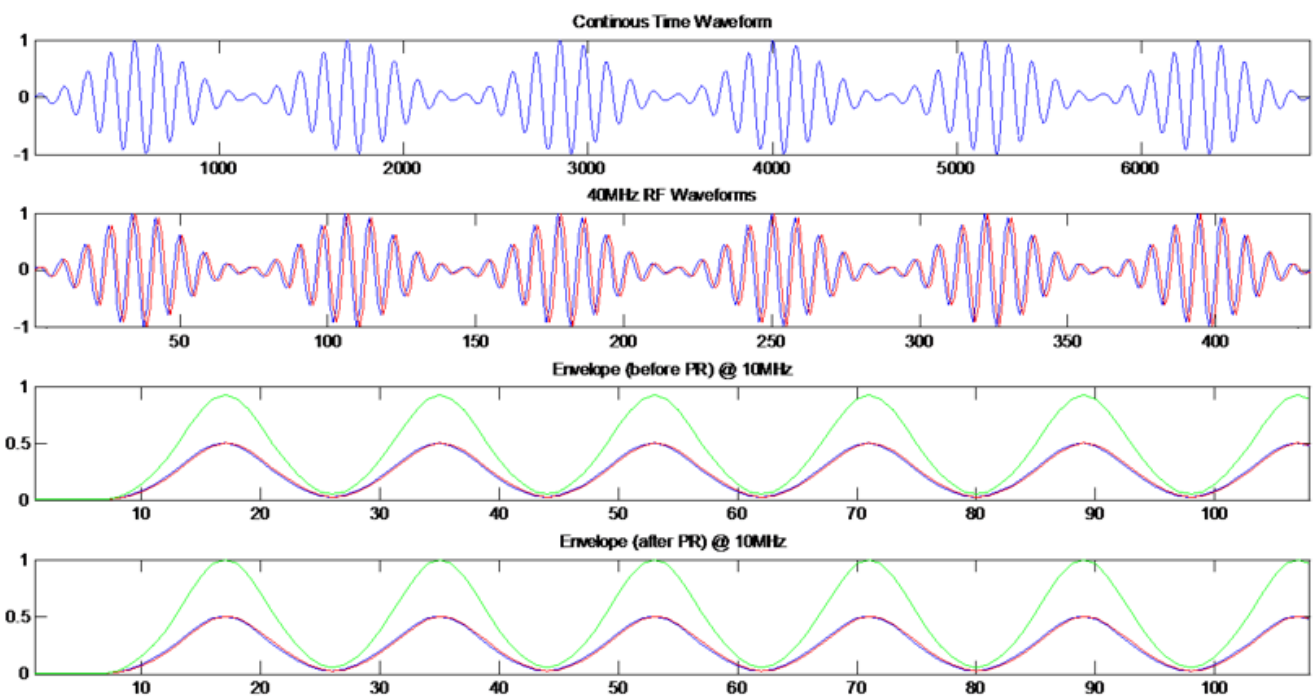

Figure 9. Delaying an Envelope Signal Using Phase Rotation

Copyright © 2015, Texas Instruments Incorporated

The two signals represented in green in these two plots indicate the effect of the phase rotation step. These signals are plotted in Figure 10. The green curve represents the envelope signal obtained before phase rotation, that is, the absolute value of the sum of the two complex signals. Since the goal of the phase rotation block is to insert a delay of 25 ns to the envelope signal D_2[m], the ideal case is where E_1[m] and E_2[m] line up exactly. Because D_1[m] = E_1[m], the ideal case can be set as the absolute value of twice D_1[m] (indicated by the blue waveform in Figure 10). To evaluate how well the phase rotation block works, this ideal waveform can be compared to the actual absolute value of the complex sum E_1[m]+ E_2[m], shown in red. As a reference, the absolute value of the complex sum D_1[m]+ D_2[m] is plotted in green. As the red and blue waveforms line up almost exactly, the functionality of the phase rotator is verified.

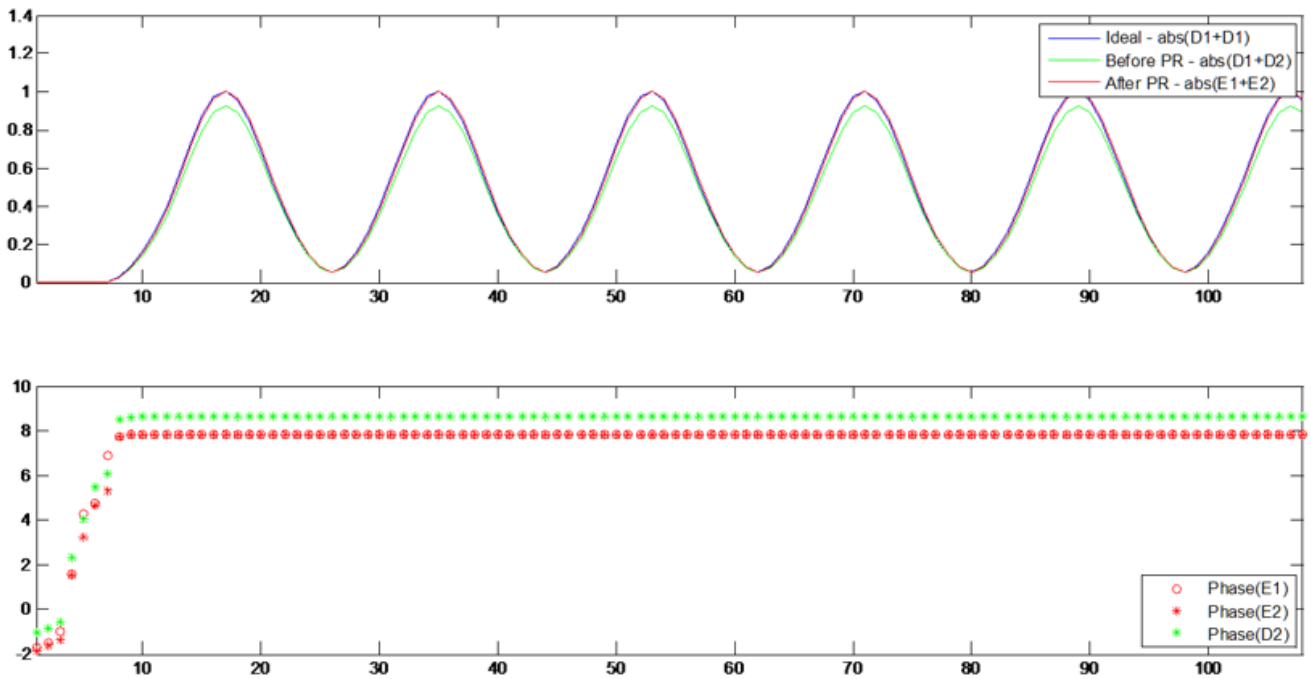

Figure 10. Waveform Comparison for Phase Rotation Beamforming

Copyright © 2015, Texas Instruments Incorporated

The beamformer system where the interpolation for fractional delay is done using a phase rotator is summarized in Figure 11.

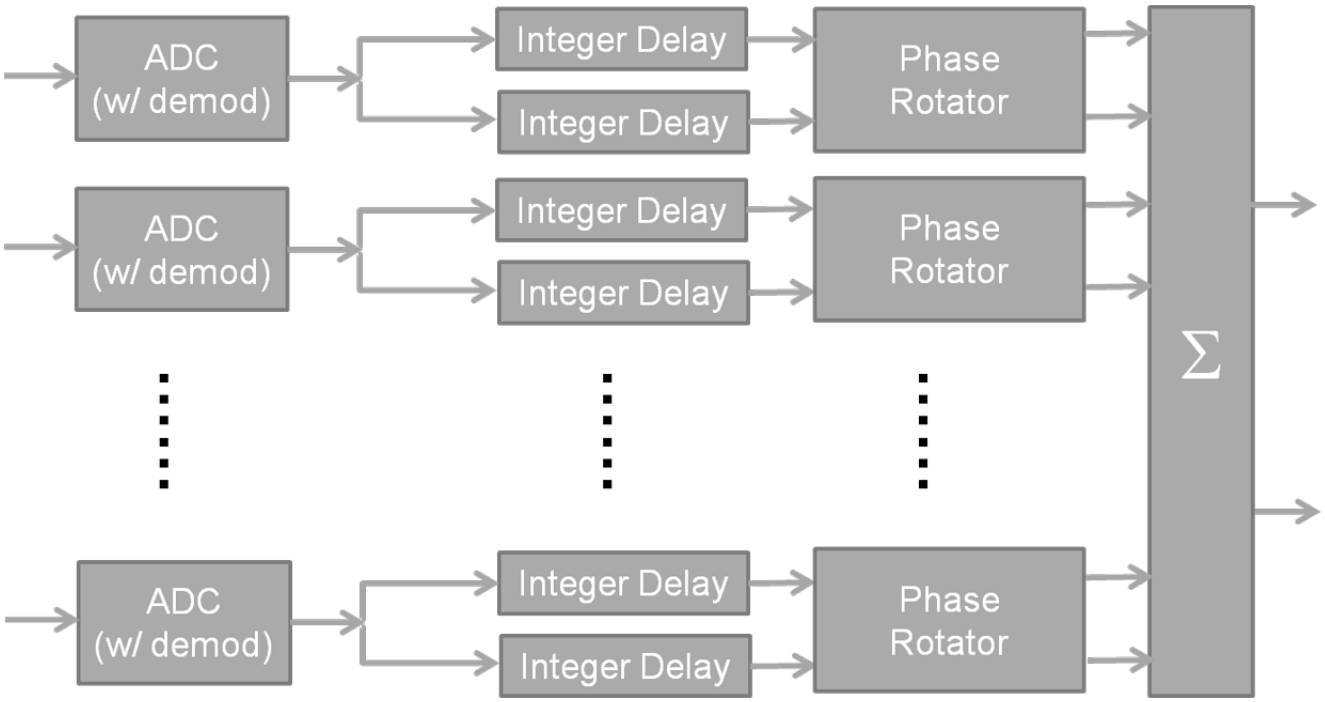

Figure 11. Demodulation Before Beamformer with Phase Rotation

Copyright © 2015, Texas Instruments Incorporated

4 AFE5809 Value Proposition for SONAR and Ultrasound Systems

This section provides an overview of the value the AFE5809 brings to a SONAR or ultrasound system through integration and digital processing.

4.1 Integration

As shown in Figure 12, the AFE5809 integrates into a single package many functions required by mid- to high-end SONAR and ultrasound systems available on the market. With these functions integrated into a single device, even next generation low-end SONAR systems could benefit from this device and drastically improve the cost, quality, and time-to-market of existing systems. More importantly, the functions provided are those found in both the front-end analog domain and the back-end digital domain of existing systems, thus reducing the overall complexity of the system.

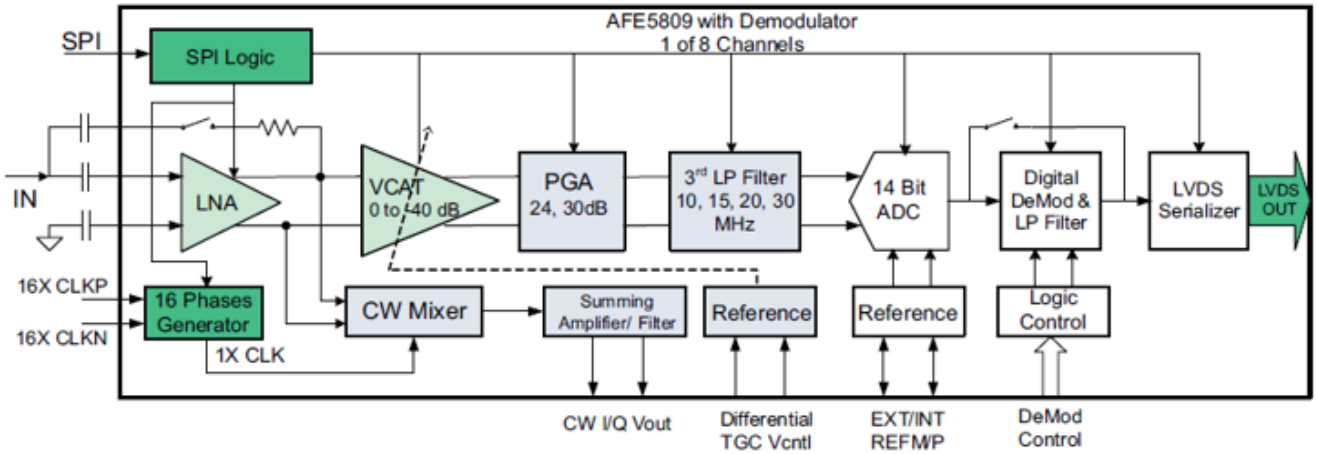

Figure 12. AFE5809 Top Level

Copyright © 2015, Texas Instruments Incorporated

As illustrated in Figure 13, the heavy back-end computational requirements to decimate and filter the output data stream can be off-loaded to the AFE5809, where decimation as high as 32 times can be implemented, in conjunction with digital FIR filtering. Further, with eight analog receiver channels available and the integration of a complex demodulator, which allows sixteen I/Q output data streams, beamforming techniques can realize spatial filtering at the transducer.

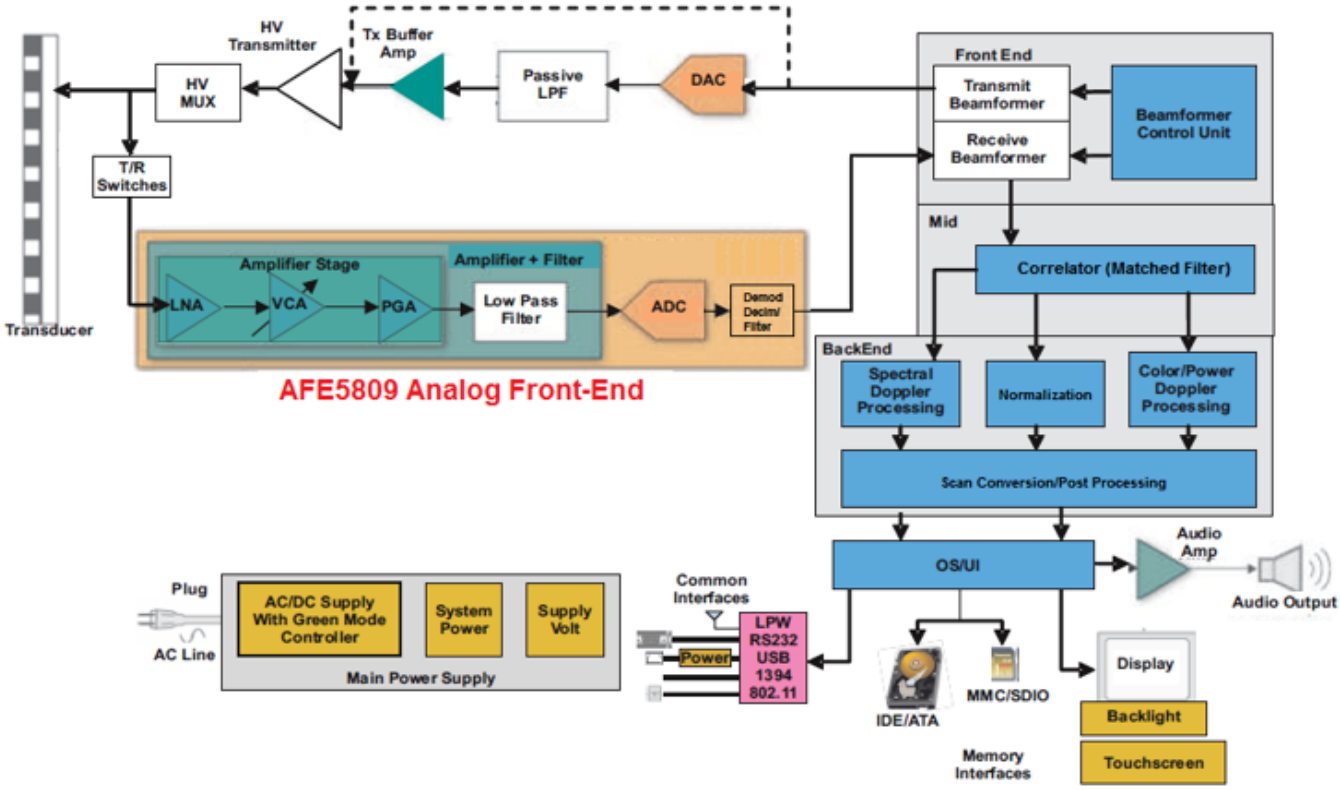

Figure 13. AFE5809 in SONAR System

Copyright © 2015, Texas Instruments Incorporated

4.2 Frequency of Operation

While medical imaging ultrasound devices typically operate in the range above 1 MHz, many SONAR systems operate in the sub-1-MHz ultrasound region with typical applications in the 100- to 500-kHz range. With proper selection of external components, the AFE5809 can process input frequencies as low as 30 kHz, as shown in Section 5.4, and as high as 32.5 MHz. The minimum sampling frequency of the AFE5809 is 10 MSPS. For conventional sonar systems, this value might seem like a high sampling frequency, but with the built-in decimation filter in the AFE5809, the effective output rate can be reduced by as much as 32 times as explained in Section 4.4.

4.3 Time Gain Control (TGC) for Dynamic Range

One of the biggest challenges with any communication system in which its environment is changing dynamically is its ability to adapt to both weak and strong signals. For a SONAR system, a strong near-field echo must be conditioned so as to not saturate and distort the receiver chain. Conversely, very weak far-field echoes must be amplified while inducing minimal noise to determine the source of the echo. To achieve this, the front-end architecture of the AFE5809 is comprised of a highly linear low noise amplifier (LNA) followed by a voltage controlled attenuator (VCAT). To minimize the reflection from the transducer to the receiver, the active termination of the LNA is programmable for a large range of input impedance covering common transducer source impedances. The variable attenuator that follows the LNA has a 40-dB dynamic range and is controlled through high bandwidth analog pins, allowing for fast control.

4.4 Decimation, Filtering, and Complex Demodulation

To take full advantage of the AFE5809 architecture, a slight variation to a conventional frequency plan is recommended. To expound on this, assume a system with a SONAR signal at 105 kHz with a 10-kHz bandwidth. The Nyquist-Shannon theorem states that sampling at 20 kHz is sufficient to replicate such a signal. However, such a system is under sampled and relies on aliasing (from the 11th Nyquist zone) to mix down the signal of interest. Since the minimum supported sampling frequency of the AFE5809 is 5 MSPS, such an approach is not viable with the AFE5809. In addition, the integrated anti-aliasing filter of the AFE5809has a minimum corner frequency of 10 MHz. Sampling below 20 MSPS fails to fully take advantage of this filter. By sampling at 20 MSPS, noise aliasing is avoided at the expense of the unwanted spectrum in the first Nyquist zone. However, this aliasing can be is alleviated by invoking the maximum decimation factor of 32, which reduces the first Nyquist frequency from 10 MHz to 312.5 kHz. Additionally, when decimating by 32, a 512th order FIR low pass filter is invoked, and the theoretical SNR improvement of 10×log (32), or 15 dB, is realized within the reduced Nyquist band of 312.5kHz. A beneficial byproduct of this architecture is that the digital receiver (probably FPGA) now has less computational burden as all, or the majority, of decimation is now performed by the AFE5809. So, while a typical sonar system would not sample at such a high rate as 20 MSPS, doing so with the AFE5809 allows the user to achieve an effective data rate that is low while also improving the resolution of the signal and interleaving LVDS data.

Copyright © 2015, Texas Instruments Incorporated

Finally, as shown in Figure 12, the AFE5809 provides a digital complex demodulator block before the decimation filter. This down mixer allows for band shifting the signal of interest to a very low frequency or baseband. Once all relevant content is shifted down to a low-frequency band, the decimation can then be more aggressive. Although this does not alleviate the sampling frequency requirement of the AFE5809 because the demodulator comes after the ADC, it does off-load such function from the digital receiver or FPGA. Also, as the mixer is complex, the I and Q vectors required by the inverse beam former in the receiver are generated, for a total of sixteen output channels, instead of the normal eight. These I/Q signals can be used in the back-end system to construct the envelope of the received echo with the minimum data required.

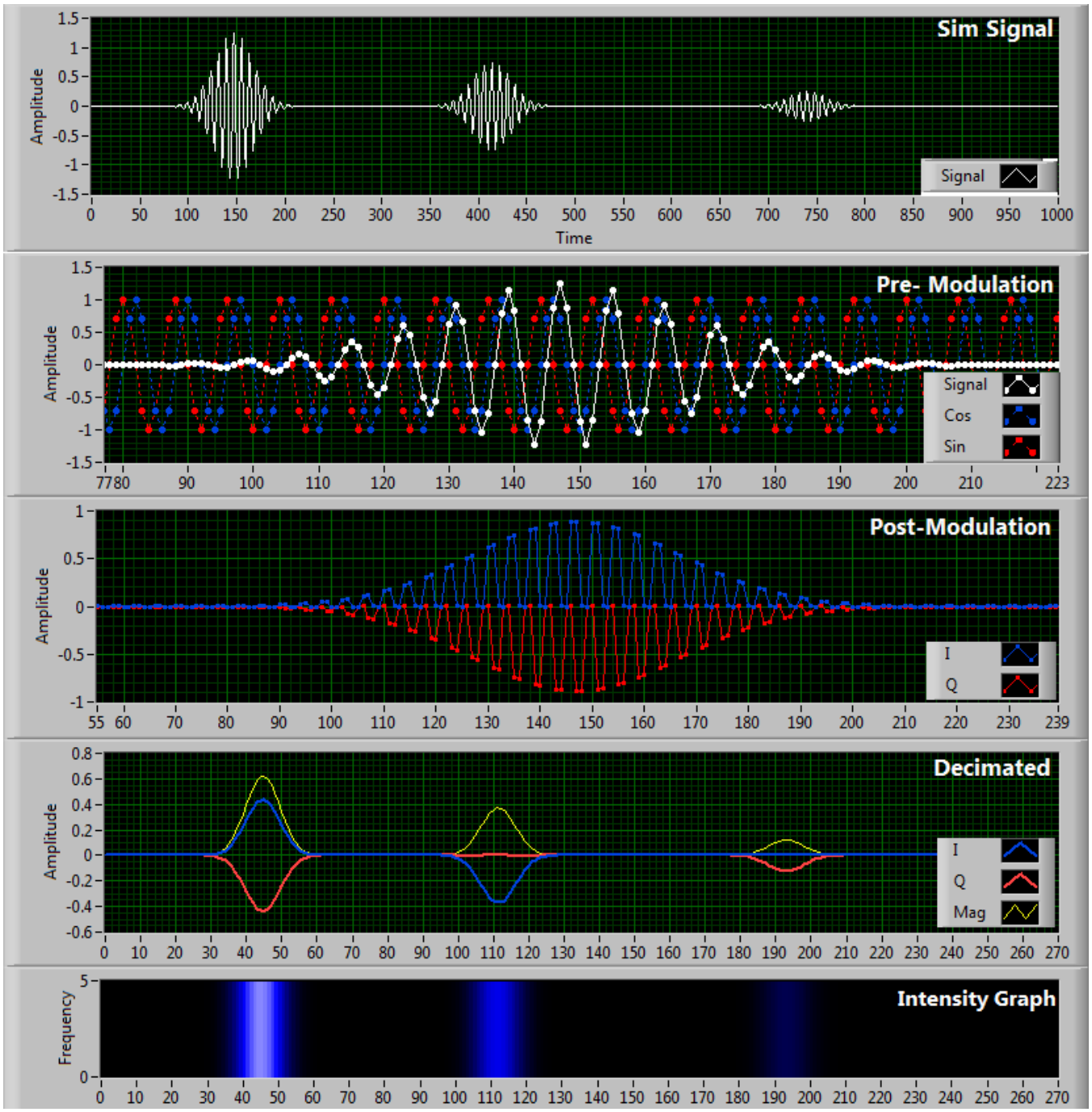

Figure 14. Simulation of AFE5809 Demodulated and Decimated Echo Train

Copyright © 2015, Texas Instruments Incorporated

To further illustrate these benefits, assume a sonar signal with a 500-kHz ±50-kHz frequency content. This signal translates to a minimum Nyquist frequency of 550 kHz if aliasing is not used, corresponding to a minimum sampling frequency of 1.1 MSPS. Despite the fact that the minimum supported sampling frequency of the AF5809 is 5 MSPS, sampling at such low frequencies fails to fully benefit from the integrated anti-aliasing filter before the ADC since its minimum corner frequency is 10 MHz. By sampling at 20 MHz, noise aliasing is avoided at the expense of the unwanted spectrum in the first Nyquist zone. With the AFE5809, the user would sample at 20 MSPS using the 10-MHz anti-alias filter, and then decimate by 18 to achieve an effective rate of 1.111 MSPS, with a theoretical 12.6-dB improvement in SNR and eight output channels of in-phase data transmitted on eight LVDS lanes. Alternatively, the user can use the demodulator feature to shift the 500-kHz signal down to baseband, or 0 Hz, with frequency content spanning from –50 to 50 kHz. Now, the required bandwidth of the digitized output data is reduced from 550 kHz to 50 kHz. Therefore, the decimation factor can be increased to 32, to achieve an effective data rate of 625 kSPS with a theoretical 15-dB improvement in SNR. Additionally, in this case, the demodulator is used and, therefore, the output data will be complex, having both I and Q elements for each channel and transmitted on only four LVDS lanes.

4.5 Output Data Compression

At the output of the AFE5809 is the LVDS serializer where the number of LVDS outputs is optimized for a given configuration. For example, when I/Q demodulation and decimation by 32 is configured, the eight LVDS outputs will be compressed onto only four LVDS outputs. Once again, this reduces the requirements of the digital receiver by halving the number of deserializers required in the FPGA. Table 1 from the AFE5809 datasheet [1] describes LVDS channel compression in detail.

Table 1. Channel Selection[(1)]

DECIMATION FACTOR (M)	MODULATE BYPASS	OUTPUT CHANNEL SELECT	FULL LVDS MODE	DECIMATION FACTOR (M)	LVDS OUTPUT DESCRIPTION
M ≥ 2	0	0	0	M < 4	LVDS1: A.I, A.Q, (zeros)
					LVDS2: B.I, B.Q, (zeros)
					LVDS3: C.I, C.Q, (zeros)
					LVDS4: D.I, D.Q, (zeros)
				M ≥ 4	LVDS1: A.I, A.Q, B.I, B.Q, (zeros) LVDS2: idle
					LVDS3: C.I, C.Q, D.I, D.Q, (zeros) LVDS4: idle
			1	X	LVDS1: A.I, A.Q, (zeros)
					LVDS2: B.I, B.Q, (zeros)
					LVDS3: C.I, C.Q, (zeros)
					LVDS4: D.I, D.Q, (zeros)
		1	0	M < 4	LVDS1: B.I, B.Q, (zeros)
					LVDS2: A.I, A.Q, (zeros)
					LVDS3: D.I, D.Q, (zeros)
					LVDS4: C.I, C.Q, (zeros)
				M ≥ 4	LVDS1: B.I, B.Q, A.I, A.Q, (zeros)
					LVDS2: idle
					LVDS3: D.I, D.Q, C.I, C.Q, (zeros)
					LVDS4: idle
			1	X	LVDS1: B.I, B.Q, (zeros)
					LVDS2: A.I, A.Q, (zeros)
					LVDS3: D.I, D.Q, (zeros)
					LVDS4: C.I, C.Q, (zeros)

(1) This table refers to individual demodulator subchip, which has four LVDS outputs, that is LVDS1 through LVDS4; and four input CHs, that is CH.A to CH.D..

Copyright © 2015, Texas Instruments Incorporated

Table 1. Channel Selection[(1)] (continued)

DECIMATION FACTOR (M)	MODULATE BYPASS	OUTPUT CHANNEL SELECT	FULL LVDS MODE	DECIMATION FACTOR (M)	LVDS OUTPUT DESCRIPTION
M ≥ 2	1	0	X	X	LVDS1: A.I; Note: the same A.I is repeated by M times.
					LVDS2: A.Q; Note: the same A.Q is repeated by M times.
					LVDS3: C.I; Note: the same C.I is repeated by M times.
					LVDS4: C.Q; Note: the same C.Q is repeated by M times.
		1	X	X	LVDS1: B.I; Note: the same B.I is repeated by M times.
					LVDS2: B.Q; Note: the same B.Q is repeated by M times.
					LVDS3: D.I; Note: the same D.I is repeated by M times.
					LVDS4: D.Q; Note: the same D.Q is repeated by M times.
M = 1	0	0	X	1	LVDS1: A.I; LVDS2: B.I; LVDS3: C.I; LVDS4: D.I
M = 1	0	1	X	1	LVDS1: B.I; LVDS2: A.I; LVDS3: D.I; LVDS4: C.I
M = 1	1	0	X	1	LVDS1: A.I; LVDS2: A.Q; LVDS3: C.I; LVDS4: C.Q
M = 1	1	1	X	1	LVDS1: B.I; LVDS2: B.Q; LVDS3: D.I; LVDS4: D.Q

Copyright © 2015, Texas Instruments Incorporated

5 Test Outline

This section describes the required equipment and signal configuration used to obtain the SONAR data and ultrasound envelope detection. The first test will seek to prove that in-phase data (no I/Q demodulation) at 200 kHz can sampled at a high rate such as 20 MSPS and then heavily decimated to both reduce computational rates at the system back-end and improve the SNR of the signal through decimation filtering. This test does not employ the I/Q demodulator due to already low frequency range of typical sonar systems. However, some SONAR systems that might operate at higher frequencies, such as 500 kHz, might employ the down conversion feature to maximize the decimation, as well as potential use the demodulator for beamforming. The second test will seek to prove the utility of the AFE5809 in envelope detection using the I/Q demodulator for beamforming with a 5-MHz sine wave burst sampled at 40 MSPS.

5.1 Test Setup and Equipment

Use the following equipment to properly demonstrate the use of the AFE5809 EVM in SONAR testing (see Figure 15):

- AFE5809EVM with USB cable and power supply cable
  - AFE5809EVM GUI and user guide found here: AFE5809 GUI
- TSW1400EVM with USB cable and supplied power supply adapter
  - TSW1400EVM GUI and user guide found here: HSDCPro
- Clock generator to produce a low-jitter 20-MHz sine or square signal at +9 dBm. This will be the A/D sampling clock.
- Trigger generator generating a rising edge (square wave or pulse) at 5-ms interval
- Low-noise sine wave generator at 200 kHz and –30 dBm, with a source impedance of 50 ohms
- 200-kHz band-pass filter to reduce out-of-band noise and harmonics from the 200-kHz sine generator
- All signal generators must be clock synchronized

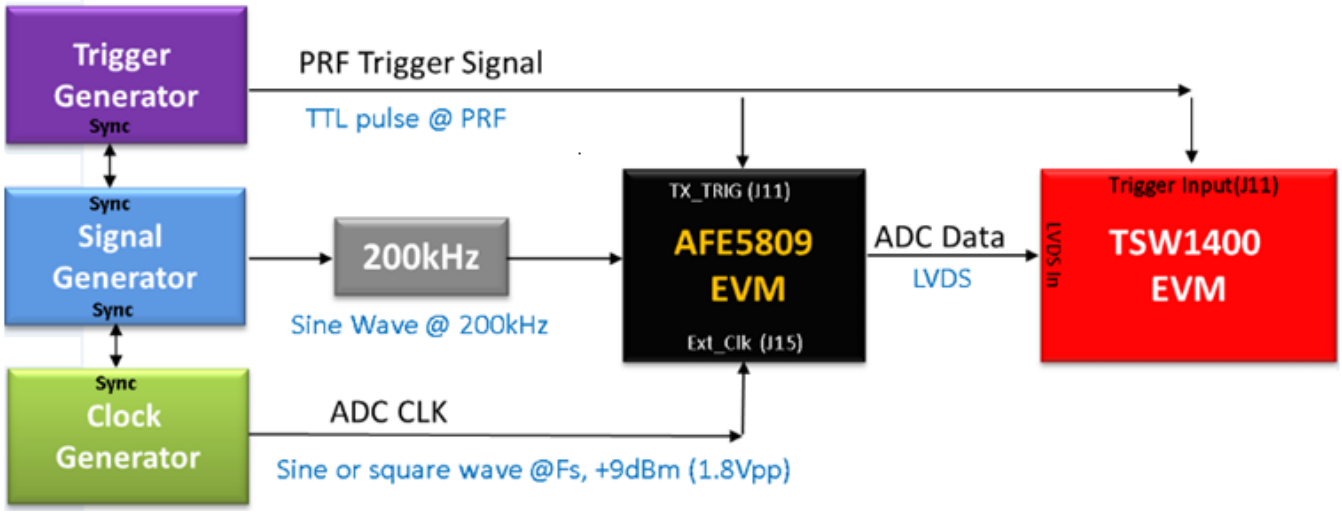

Figure 15. Block Diagram of Sonar Setup

Copyright © 2015, Texas Instruments Incorporated

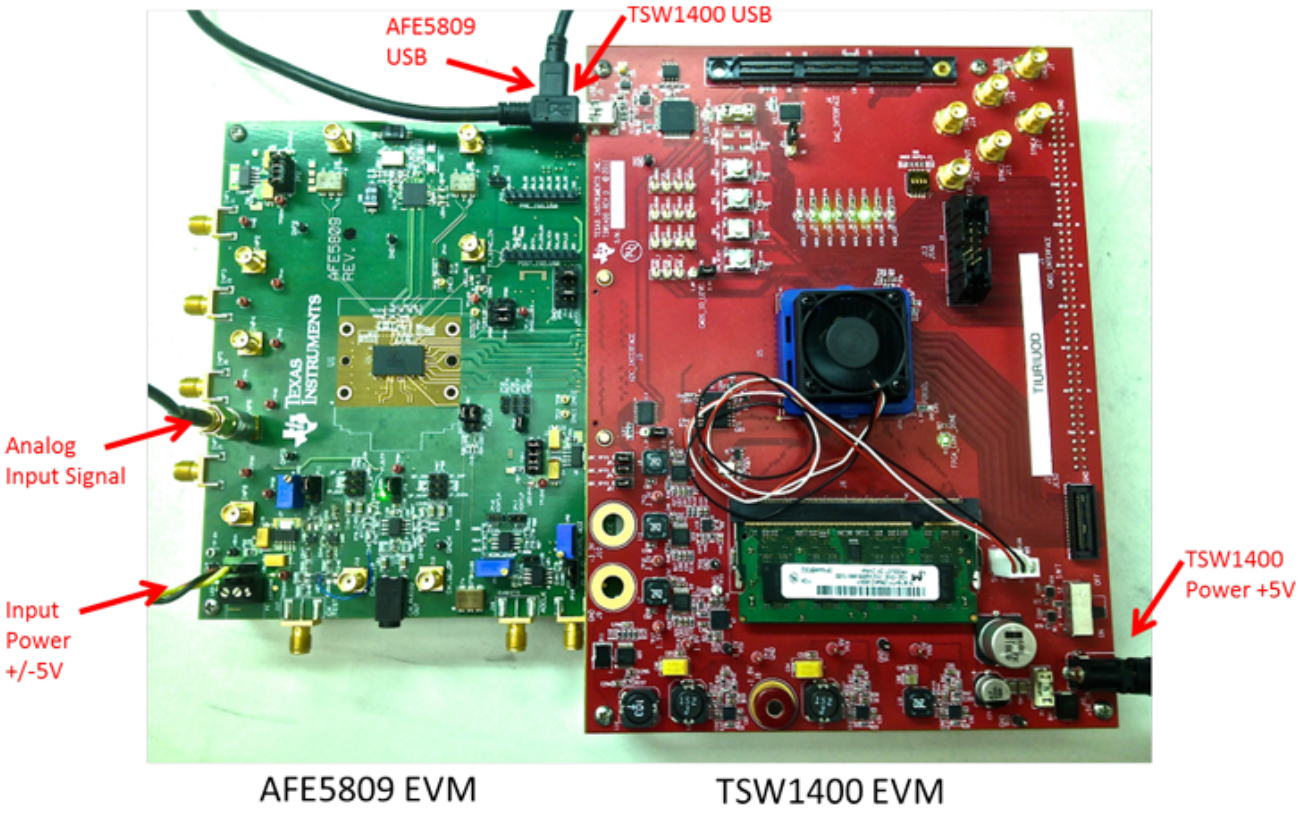

Figure 16. EVM Setup

The generators used for this experiment are the following:

- Signal generator and trigger generator: AP SYS-2722 24-bit DAQ, used to a clean signal in the SONAR band.
- Clock generator: Agilent E4428C

Copyright © 2015, Texas Instruments Incorporated

5.2 Envelope Detection Test Setup and Equipment

Use the following equipment to properly demonstrate the use of the AFE5809 EVM in SONAR testing (see Figure 17):

- AFE5809EVM with USB cable and power supply cable
  - AFE5809EVM GUI and user guide found here: AFE5809EVM
- TSW1400EVM with USB cable and supplied power supply adapter
  - TSW1400EVM GUI and user guide found here: HSDCPro GUI
- Clock generator to produce a low-jitter 40-MHz sine or square signal at +9 dBm
- Trigger generator generating a rising edge (square wave or pulse) at 5-ms interval
- Arbitrary function generator or signal generator to produce a 5-MHz sine burst repeated at a regular interval. This is used to mimic the echo received on the transducer
- All signal generators must be clock synchronized

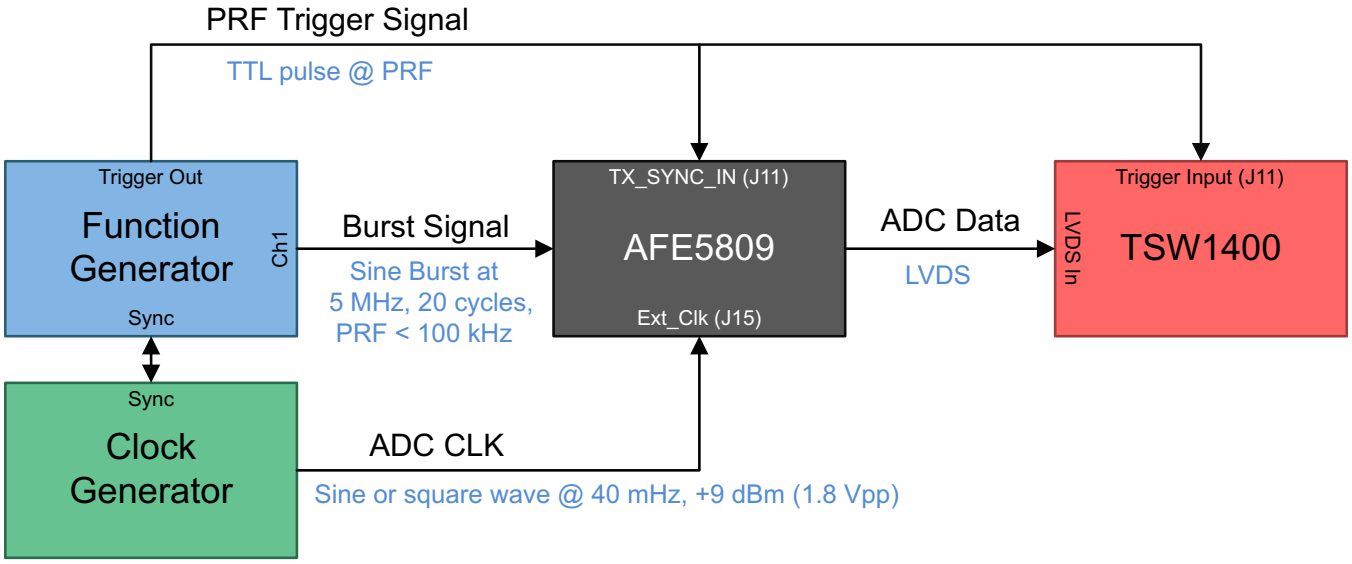

Figure 17. Block Diagram of Envelope Detection

This experiment used the following generators:

- Tektronix: AFG3102 CH1, used to simulate the modulated echo input signal.
- Clock generator: AFG3102 CH2, used for the A/D sampling clock.
- Trigger generator: AFG3102 trigger output, used to trigger both the FPGA data capture, as well to trigger the DEMOD block in the AFE5809.

Copyright © 2015, Texas Instruments Incorporated

5.3 AFE5809 EVM Modification for Low Frequency Support

Configuring the EVM for low frequency support requires three steps:

1. Change the AC coupling capacitor for any desired analog input channel.
2. Disable PGA integrator in the AFE5809 (Reg. 51[4] = '1').
3. Set AFE5809 HPF to the 50-kHz setting in the GUI (Reg. 59[3:2] = '01').

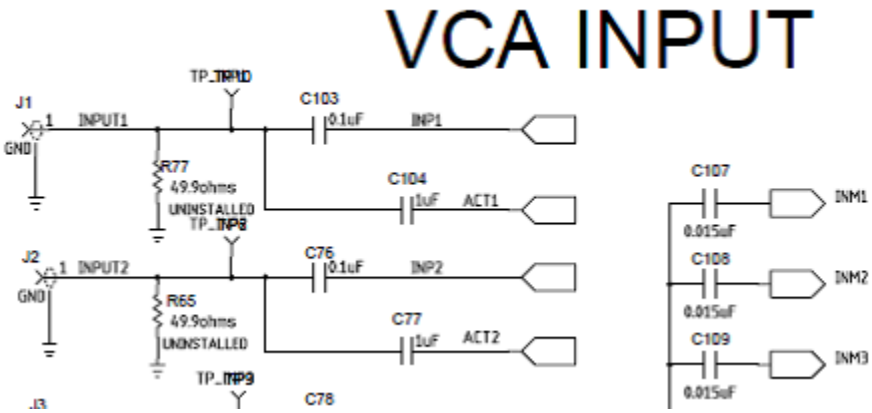

Figure 18. LNA Input AC Coupling Setup

The input capacitor configuration required for sonar applications is:

- C_INP = 1 µF
- C_INM = 1 µF
- C_ACT = 1 µF
- R_TERM = 50 Ω

5.4 Measure HPF

Verify the transfer function of the expected high-pass filter to ensure that the device does not filter any desired signals. While the device is typically configured for ultrasound applications where a higher filter cut-off frequency is desired, the AC coupling capacitance of the LNA input was increased to lower this HPF cut-off frequency. The desired cut-off frequency for this test will be 50 kHz.

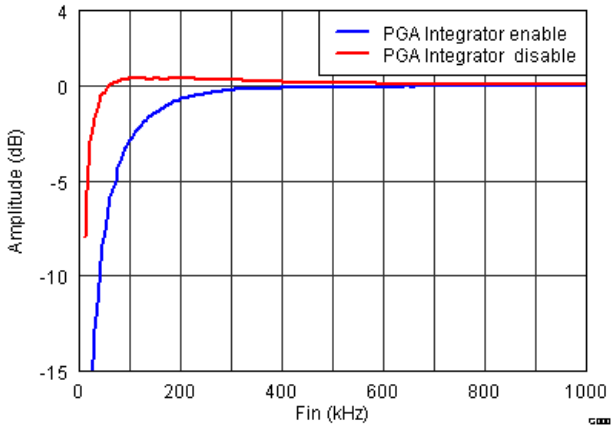

Figure 19. Signal Chain Low Frequency Response With INM Capacitor = 1 µF

Copyright © 2015, Texas Instruments Incorporated

5.5 SNR Measurement Before and After Decimation

Compare the SNR performance before and after decimation, as the decimation filter is expected to improve SNR by the factor 10×log(M), where M is the decimation factor. For the SNR measurement, an FFT with a rectangular window with coherent sampling is required. The HSDCPro FFT display will help to analyze the frequency content of the signal.

5.6 Demod Configuration for SNR Measurement

As shown in Figure 20, the demod block of the AFE5809 is split into independent sub-blocks, where only the decimation and channel multiplexing blocks are used in this sonar application example. As mentioned before, the user can also incorporate the down conversion block if needed.

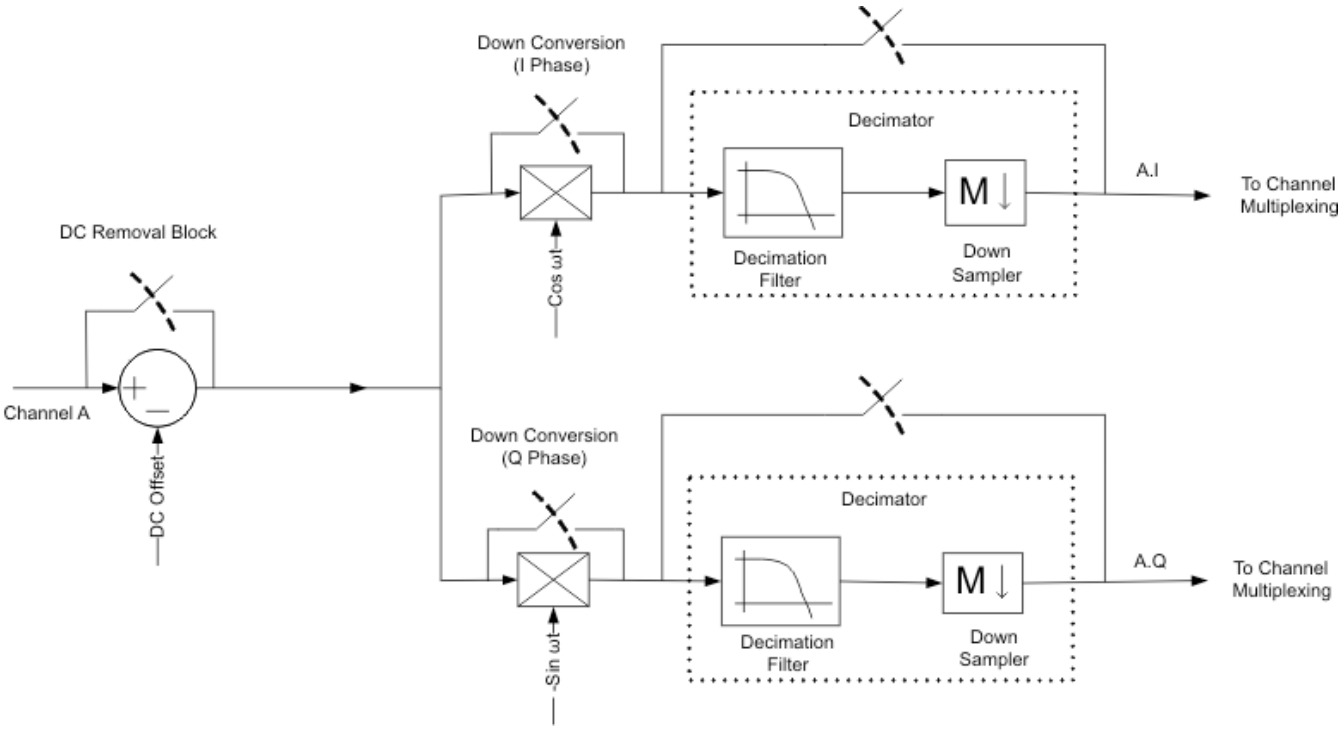

Figure 20. Signal Chain of Demodulator Sub-Blocks

Copyright © 2015, Texas Instruments Incorporated

In the GUI, configure the AFE5809 as shown in Figure 21:

- DC removal block bypassed
- Down conversion block bypassed
- Dec_bypass disabled
- Dec_Shift_Force enabled and set to 7
- Dec_Shift_Scale enabled
- Manual start coefficient enabled and set to 0
- Manual decimation factor enabled and set to 32
- DHPF enabled

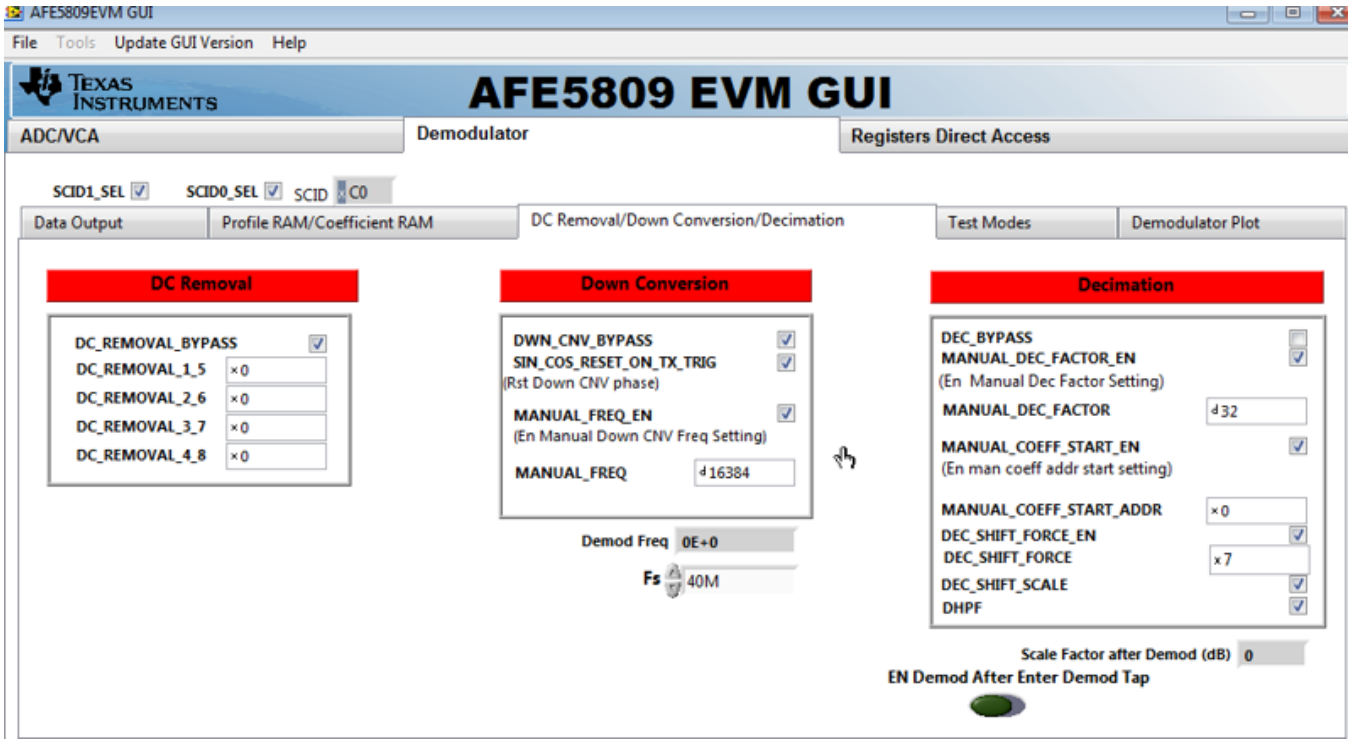

Figure 21. GUI: Decimation Configuration

Copyright © 2015, Texas Instruments Incorporated

6 Test Data

6.1 SNR Improvement

Figure 22 shows the FFT of the signal without any decimation. The 200-kHz signal in the 10-MHz Nyquist shows an SNR of 70.90 dBFs. By sampling at 20 MHz, the user takes full advantage of the 10-MHz analog
anti-aliasing filter in the VCA section of the AFE5809. However, most of this spectrum is unused for sonar applications.

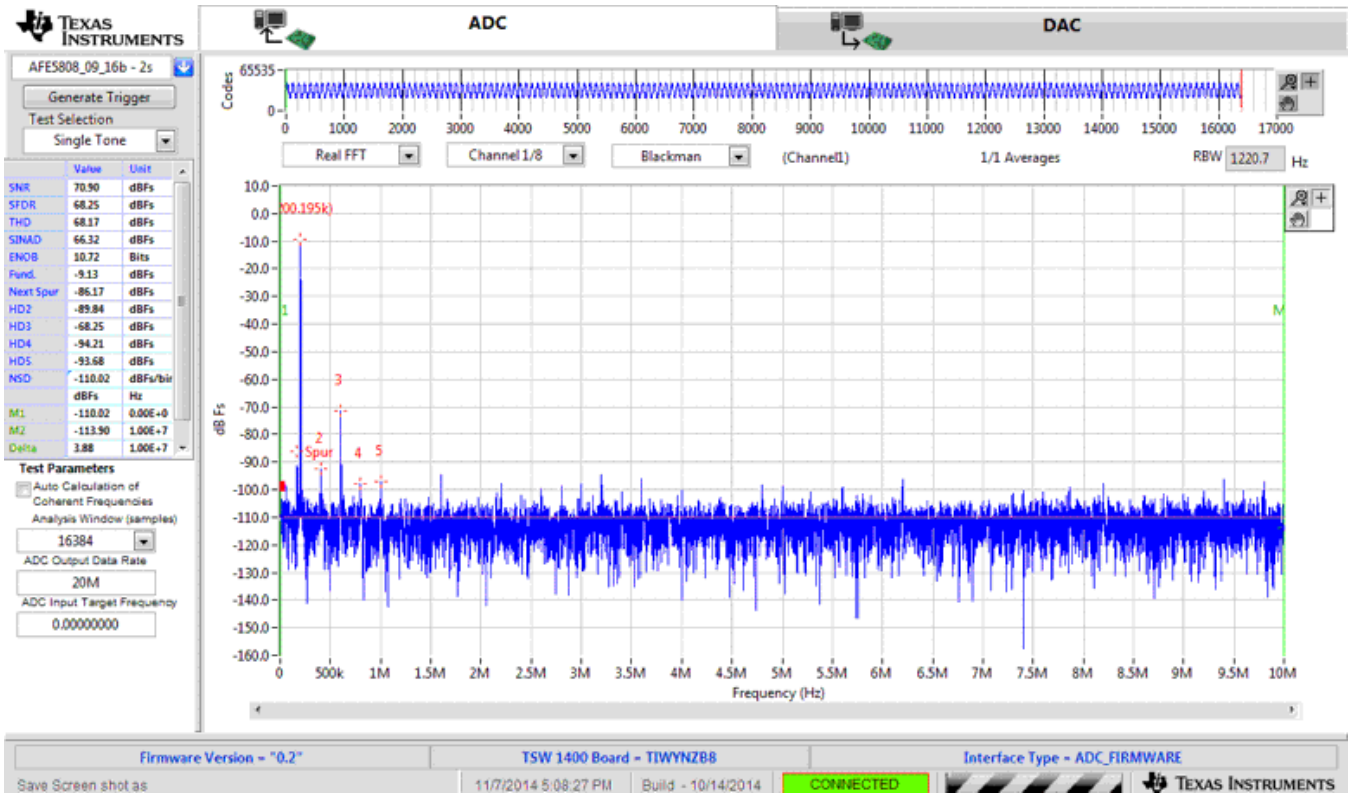

Figure 22. FFT 200-kHz Signal at 20 MSPS With No Decimation

Copyright © 2015, Texas Instruments Incorporated

It is possible to remove most of this unused bandwidth with an internal decimation of factor 32. With this new factor, the 10-MHz Nyquist frequency is now moved down to 312.5 kHz, which still allows the 200-kHz signal. The effective data rate is reduced from 20 MHz to 625 kHz, and the new Nyquist is 312.5 kHz. All the relevant frequency content is maintained in this bandwidth. The SNR is improved by the decimation filter to 83.6 dBFs. Therefore, our SNR improvement with a decimation of 32 is 12.7 dB as shown in Figure 23. The fundamental signal is shown at 200kHz, and an artifact from the signal generator is shown at about 170kHz. This can be ignored.

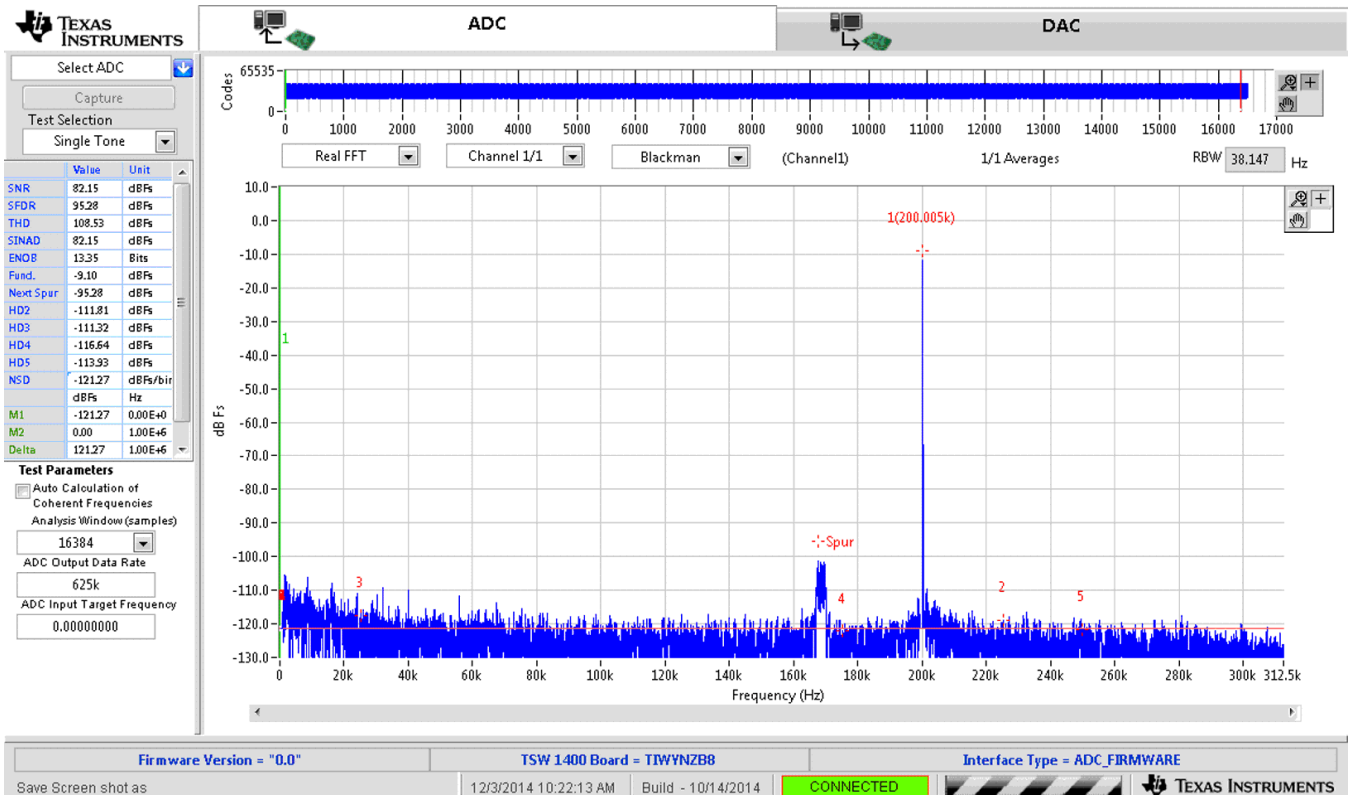

Figure 23. FFT 200-kHz Signal Sampled at 20 MSPS With Decimation = 32

Copyright © 2015, Texas Instruments Incorporated

6.2 Envelope Detection

To demonstrate envelope detection with the AFE5809, first generate a periodic sine burst waveform at 5 MHz using the function generator, and use this function generator as the analog input signal to the AFE. Figure 24 is a data capture of the AFE output data in the TSW1400 tool, HSDCPro. This capture is a simple digitization at 40 MSPS of the signal with no demodulation or decimation.

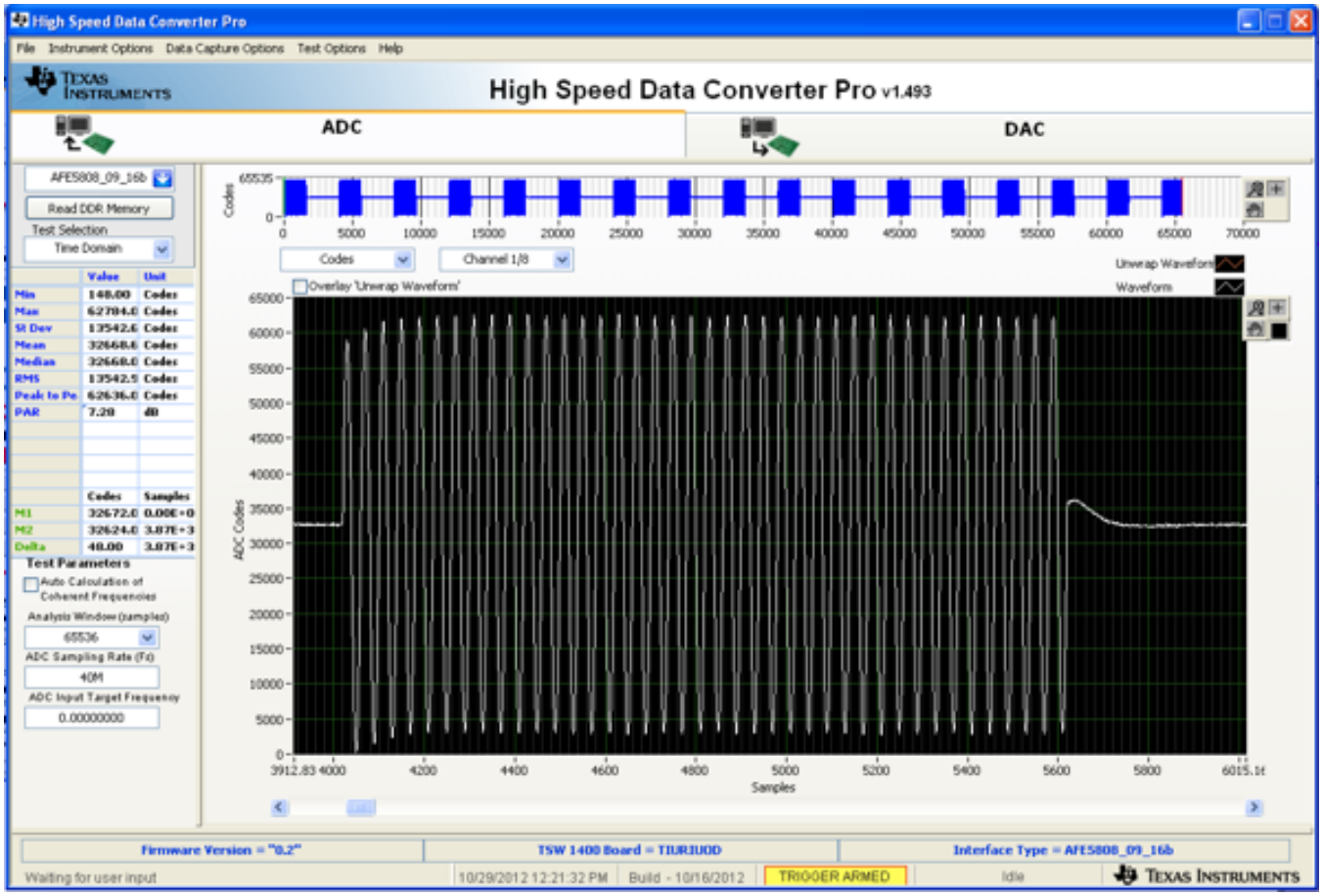

Figure 24. Sine Burst Waveform at Frequency of 5 MHz (Fs/8, where Fs=40MSPS)

In , The data is first mixed with 5 MHz sine and cosine waves internal on the AFE5809, and is then decimated by 4. The resulting waveform shows interleaved data that contain both the In-phase and Quadrature-phase elements of the envelope. The sync pattern required for data separation is also seen.

Copyright © 2015, Texas Instruments Incorporated

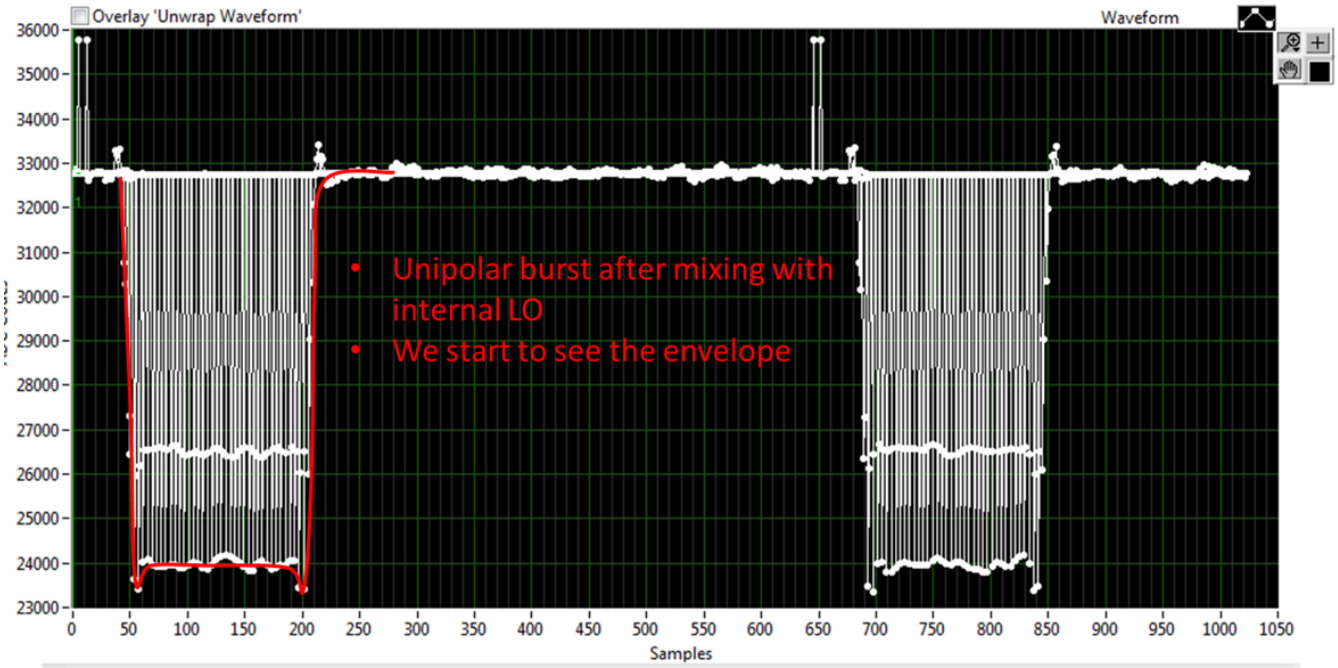

Figure 25. AFE5809 LVDS Output for Sine Burst After I/Q Demodulation at Fs/8 and Decimation of 4

In Figure 26, a closer look at the data reveals the interleaving structure. Both I and Q from two channels can be compressed onto one LVDS lane for denser data transport to the FPGA. In this example, 8 channels of I and Q data can be transmitted on 4 LVDS lanes. In Figure 27, we can see that the data is separated into channels and then I and Q elements, so that the true envelope waveform appears.

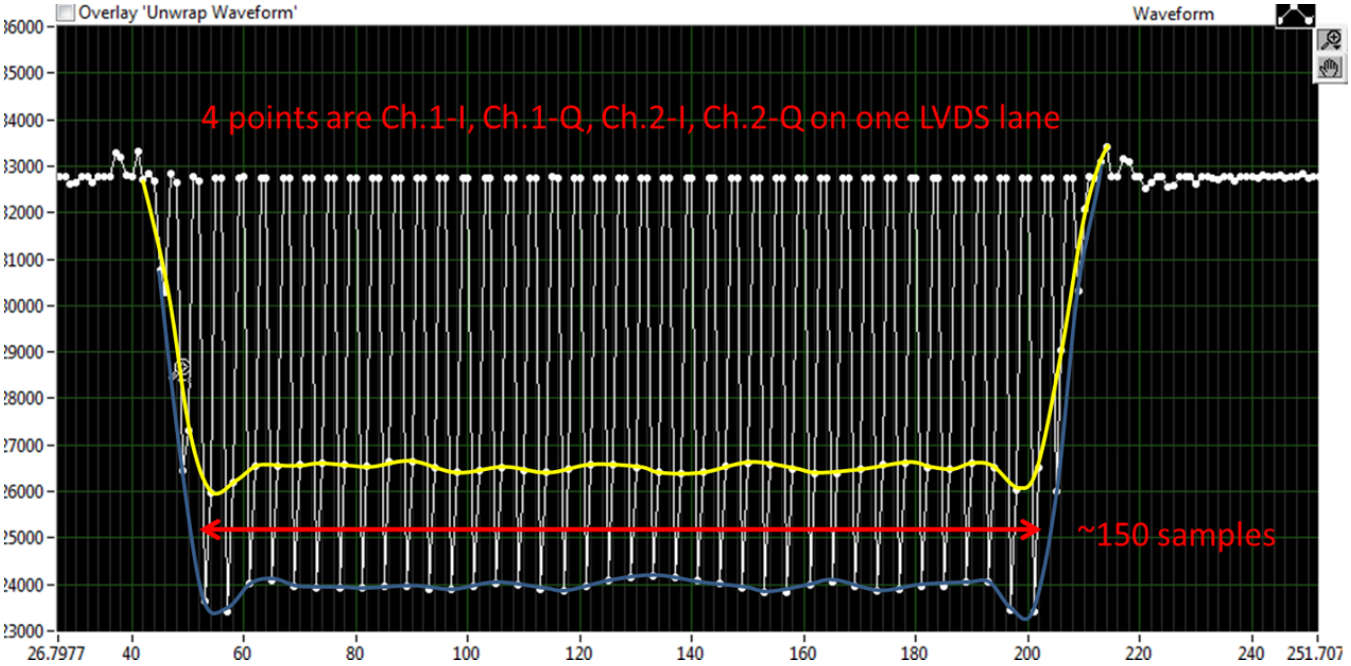

Figure 26. Sine Burst After I/Q Demodulation at Fs/8 and Decimation of 4, Two Channels on One LVDS Output Lane

Copyright © 2015, Texas Instruments Incorporated

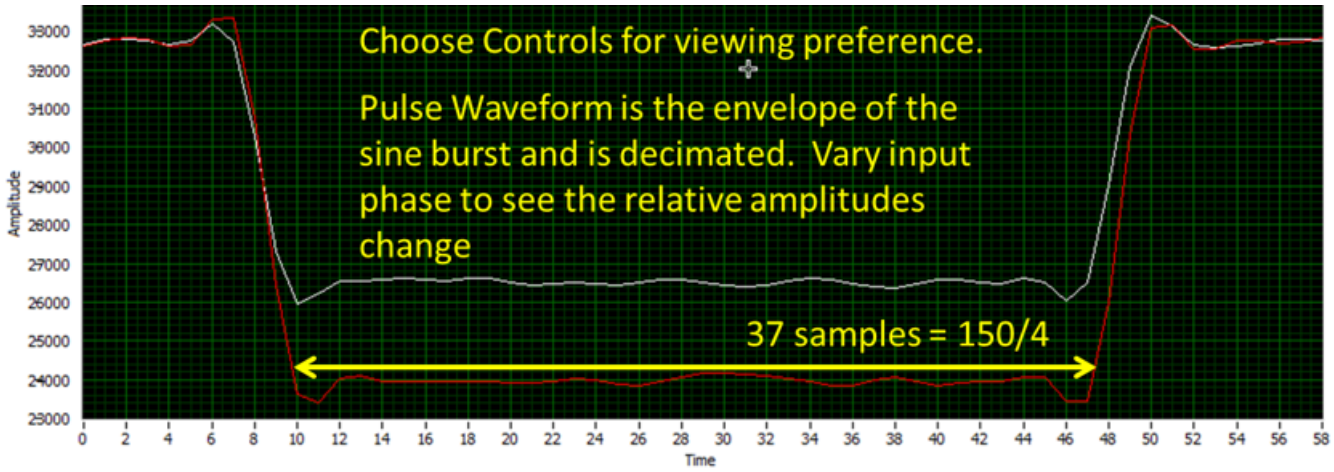

Figure 27. Separated Data After Receiver Processing Shows Decimated Envelope

Copyright © 2015, Texas Instruments Incorporated

7 Conclusion

This TI Design has reviewed the potential use of AFE5809 for SONAR RX chain applications. The theory of beam forming and its applications in multi-path signal processing have been presented. The AFE5809 features 8 channels of simultaneously sampled analog signal conditioning (LNA+VCAT+PGA) and Digital Processing (ADC + Digital Demodulator) that brings a high level of system receive path integration and enables high-performance echo-location imaging for high-end SONAR systems. Measured data at input signals of 200kHz – typical of SONAR frequencies – has been presented. The AFE5809 is ideal for SONAR RX processing since the wide-band signal chain allows high speed sampling to lower noise. This is complemented by the back-end decimation stage that allows lower data rate and boosted SNR. The SNR improvement achieved by applying decimation allows signals (i.e. echoes) in the SONAR frequency band to be digitized without degradation. Finally, measurement results that prove the envelope detection capability of the AFE5809 have also been presented.

Copyright © 2015, Texas Instruments Incorporated

8 References

1. Texas Instruments, *Fully Integrated, 8-Channel Ultrasound Analog Front End With Passive CW Mixer, and Digital I/Q Demodulator, 0.75 nV/rtHz, 14, 12-Bit, 65 MSPS, 158 mW/CH*, AFE5809 Datasheet (SLOS738).
2. C. Gao, L. Zhang, E.M.C. Wong, *Design of a digital phase shift beamformer for ultrasonic imaging*, 2004 IEEE International Workshop on Biomedical Circuits and Systems, vol., no., pp. S2/2–13-6, 1–3 Dec. 2004.
3. A. Agarwal, Y. M. Yoo, F.K. Schneider, C. Gao, L. M. Koh, Y. Kim, *New Demodulation Method for Efficient Phase-Rotation-Based Beamforming*, IEEE Transactions on Ultrasonics, Ferroelectrics and Frequency Control, vol.54, no.8, pp.1656–1668, August 2007.

9 About the Author

CHUCK SMYTH is an Applications Engineer at Texas Instruments in the TI Healthtech department, focusing on ultrasound imaging products, specifically the AFE analog-front ends. Here he develops and builds reference evaluation EVMs, supports customers through the design-in process, understands market conditions in order to drive critical business decisions about new products and target end applications, trains field application engineers and customers in the use of these products for echo-location applications. He brings to this role his extensive experience in high-speed digital, low-noise analog and mixed-signal design. Chuck received his Master of Science in Electrical Engineering (MSEE) from the University of Florida in Gainesville,FL.

CHRISTIAN YOTS is an Applications Engineer at Texas Instruments in the TI Healthtech department, focusing on ultrasound imaging products, specifically the AFE analog-front ends. Christian joined TI in 1993 after receiving a Bachelor of Science in Electrical Engineering (BSEE) from Auburn University. He earned a Masters of Science in Electrical Engineering from University of Texas at Arlington in 1997. His 22 year career at TI includes roles as IC process, product, test, characterization, systems, applications, and design engineer. His extensive experience includes development of the leading edge communication transceivers in cellular telephony, WIFI, and microwave backhaul systems. In his current role, he develops software and hardware tools to promote, evaluate, and design-in TI's ADC and AFE portfolio.

BONNIE LAM is a PhD student in The Energy-Efficient Integrated Circuits and Systems Group at the Massachusetts Institute of Technology. Her research interests are in digital design methodologies for low-power applications and ow-power techniques for ultrasound imaging. She received her Masters of Science (M.S.) degree in Electrical Engineering and Computer Science from Massachusetts Institute of Technology in 2010.

Copyright © 2015, Texas Instruments Incorporated

IMPORTANT NOTICE FOR TI REFERENCE DESIGNS

Texas Instruments Incorporated ("TI") reference designs are solely intended to assist designers (“Buyers”) who are developing systems that incorporate TI semiconductor products (also referred to herein as “components”). Buyer understands and agrees that Buyer remains responsible for using its independent analysis, evaluation and judgment in designing Buyer’s systems and products.

TI reference designs have been created using standard laboratory conditions and engineering practices. **TI has not conducted any testing other than that specifically described in the published documentation for a particular reference design.** TI may make corrections, enhancements, improvements and other changes to its reference designs.

Buyers are authorized to use TI reference designs with the TI component(s) identified in each particular reference design and to modify the reference design in the development of their end products. HOWEVER, NO OTHER LICENSE, EXPRESS OR IMPLIED, BY ESTOPPEL OR OTHERWISE TO ANY OTHER TI INTELLECTUAL PROPERTY RIGHT, AND NO LICENSE TO ANY THIRD PARTY TECHNOLOGY OR INTELLECTUAL PROPERTY RIGHT, IS GRANTED HEREIN, including but not limited to any patent right, copyright, mask work right, or other intellectual property right relating to any combination, machine, or process in which TI components or services are used. Information published by TI regarding third-party products or services does not constitute a license to use such products or services, or a warranty or endorsement thereof. Use of such information may require a license from a third party under the patents or other intellectual property of the third party, or a license from TI under the patents or other intellectual property of TI.

TI REFERENCE DESIGNS ARE PROVIDED "AS IS". TI MAKES NO WARRANTIES OR REPRESENTATIONS WITH REGARD TO THE REFERENCE DESIGNS OR USE OF THE REFERENCE DESIGNS, EXPRESS, IMPLIED OR STATUTORY, INCLUDING ACCURACY OR COMPLETENESS. TI DISCLAIMS ANY WARRANTY OF TITLE AND ANY IMPLIED WARRANTIES OF MERCHANTABILITY, FITNESS FOR A PARTICULAR PURPOSE, QUIET ENJOYMENT, QUIET POSSESSION, AND NON-INFRINGEMENT OF ANY THIRD PARTY INTELLECTUAL PROPERTY RIGHTS WITH REGARD TO TI REFERENCE DESIGNS OR USE THEREOF. TI SHALL NOT BE LIABLE FOR AND SHALL NOT DEFEND OR INDEMNIFY BUYERS AGAINST ANY THIRD PARTY INFRINGEMENT CLAIM THAT RELATES TO OR IS BASED ON A COMBINATION OF COMPONENTS PROVIDED IN A TI REFERENCE DESIGN. IN NO EVENT SHALL TI BE LIABLE FOR ANY ACTUAL, SPECIAL, INCIDENTAL, CONSEQUENTIAL OR INDIRECT DAMAGES, HOWEVER CAUSED, ON ANY THEORY OF LIABILITY AND WHETHER OR NOT TI HAS BEEN ADVISED OF THE POSSIBILITY OF SUCH DAMAGES, ARISING IN ANY WAY OUT OF TI REFERENCE DESIGNS OR BUYER’S USE OF TI REFERENCE DESIGNS.

TI reserves the right to make corrections, enhancements, improvements and other changes to its semiconductor products and services per JESD46, latest issue, and to discontinue any product or service per JESD48, latest issue. Buyers should obtain the latest relevant information before placing orders and should verify that such information is current and complete. All semiconductor products are sold subject to TI’s terms and conditions of sale supplied at the time of order acknowledgment.

TI warrants performance of its components to the specifications applicable at the time of sale, in accordance with the warranty in TI’s terms and conditions of sale of semiconductor products. Testing and other quality control techniques for TI components are used to the extent TI deems necessary to support this warranty. Except where mandated by applicable law, testing of all parameters of each component is not necessarily performed.

TI assumes no liability for applications assistance or the design of Buyers’ products. Buyers are responsible for their products and applications using TI components. To minimize the risks associated with Buyers’ products and applications, Buyers should provide adequate design and operating safeguards.

Reproduction of significant portions of TI information in TI data books, data sheets or reference designs is permissible only if reproduction is without alteration and is accompanied by all associated warranties, conditions, limitations, and notices. TI is not responsible or liable for such altered documentation. Information of third parties may be subject to additional restrictions.

Buyer acknowledges and agrees that it is solely responsible for compliance with all legal, regulatory and safety-related requirements concerning its products, and any use of TI components in its applications, notwithstanding any applications-related information or support that may be provided by TI. Buyer represents and agrees that it has all the necessary expertise to create and implement safeguards that anticipate dangerous failures, monitor failures and their consequences, lessen the likelihood of dangerous failures and take appropriate remedial actions. Buyer will fully indemnify TI and its representatives against any damages arising out of the use of any TI components in Buyer’s safety-critical applications.

In some cases, TI components may be promoted specifically to facilitate safety-related applications. With such components, TI’s goal is to help enable customers to design and create their own end-product solutions that meet applicable functional safety standards and requirements. Nonetheless, such components are subject to these terms.

No TI components are authorized for use in FDA Class III (or similar life-critical medical equipment) unless authorized officers of the parties have executed an agreement specifically governing such use.

Only those TI components that TI has specifically designated as military grade or “enhanced plastic” are designed and intended for use in military/aerospace applications or environments. Buyer acknowledges and agrees that any military or aerospace use of TI components that have ***not*** been so designated is solely at Buyer's risk, and Buyer is solely responsible for compliance with all legal and regulatory requirements in connection with such use.

TI has specifically designated certain components as meeting ISO/TS16949 requirements, mainly for automotive use. In any case of use of non-designated products, TI will not be responsible for any failure to meet ISO/TS16949.

Mailing Address: Texas Instruments, Post Office Box 655303, Dallas, Texas 75265
Copyright © 2015, Texas Instruments Incorporated